

Universal localization-delocalization transition in chiral-symmetric Floquet drives

Adrian B. Culver,^{1,*} Pratik Sathe,^{1,2,3} Albert Brown,¹ Fenner Harper,¹ and Rahul Roy^{1,†}

¹*Mani L. Bhaumik Institute for Theoretical Physics, Department of Physics and Astronomy, University of California Los Angeles, Los Angeles, California 90095, USA*

²*Theoretical Division (T-4), Los Alamos National Laboratory, Los Alamos, New Mexico 87545, USA*

³*Information Science & Technology Institute, Los Alamos National Laboratory, Los Alamos, New Mexico 87545, USA*

(Dated: September 23, 2025)

Periodically driven systems often exhibit behavior distinct from static systems. In single-particle, static systems, any amount of disorder generically localizes all eigenstates in one dimension. In contrast, we show that in topologically nontrivial, single-particle Floquet loop drives with chiral symmetry in one dimension, a localization-delocalization transition occurs as the time t is varied within the driving period ($0 \leq t \leq T_{\text{drive}}$). We find that the time-dependent localization length $L_{\text{loc}}(t)$ diverges with a universal exponent as t approaches the midpoint of the drive: $L_{\text{loc}}(t) \sim (t - T_{\text{drive}}/2)^{-\nu}$ with $\nu = 2$. We provide analytical and numerical evidence for the universality of this exponent within the AIII symmetry class.

I. INTRODUCTION

The interplay of disorder and topology can produce localization-delocalization transitions in both undriven (static) and driven (Floquet) systems. This phenomenon is particularly prominent in low-dimensional systems, in which the tendency of disorder to lead to Anderson localization is strongest.

Let us recall an illustrative example from static systems. In the integer quantum Hall effect plateau transition [1], there is a conflict between disorder, which favors localization, and a nontrivial value of a topological index, which forbids complete localization. Indeed, the nonzero Chern number implies that each Landau band must include a delocalized state (at some energy E_c), while the remaining states are generically localized by disorder [2]. As the energy E crosses the transition point E_c , the localization length L_{loc} diverges on both sides as $L_{\text{loc}} \sim 1/|E - E_c|^\nu$ with a universal exponent ν whose precise value remains controversial [3].

In the periodic table of static topological insulators and superconductors [4], localization-delocalization transitions have been studied in various Altland-Zirnbauer symmetry classes [5–8]. In the case of the chiral-symmetric class (AIII) in one spatial dimension, a localization-delocalization transition at zero energy has been shown to accompany a topological phase transition [9] (see also Refs. [8, 10] for the 3D case). Furthermore, broader theoretical approaches to localization-delocalization transitions have been proposed, including a nonperturbative transfer-matrix method for quasi-one-dimensional systems in several symmetry classes [11] and a random Dirac Hamiltonian method for the full periodic table [12].

Localization-delocalization transitions have also been studied in Floquet systems. Examples include the Floquet topological Anderson insulator [13–15], discrete-time quantum walks [16–20] (which are closely related to Floquet systems and which have also been proposed as a means to realize static topological phases [21]), and an effective Hamiltonian theory for disorder-induced transitions from topologically nontrivial to trivial phases [22]. Let us also mention Ref. [23], which finds, in the one-dimensional driven Rice-Mele model, a transition similar to the integer quantum Hall plateau transition. Indeed, Ref. [23] finds a localization-delocalization transition from a topologically nontrivial phase to a trivial phase at a critical value of disorder strength $W = W_c$; furthermore, the localization length of the Floquet states diverges as $L_{\text{loc}} \sim (W - W_c)^{-\beta}$ with $\beta \simeq 2$.

When prior work on localization-delocalization phenomena in the Floquet (or quantum walk) case has considered symmetries [16–19, 24], the focus has generally been on the symmetries of the Floquet Hamiltonian H_F , which determines the time evolution operator for a single driving period. For instance, chiral symmetry \mathcal{C} imposes the requirement $\mathcal{C}H_F\mathcal{C}^{-1} = -H_F$ [25]. However, a full account of topological possibilities in Floquet systems requires consideration of further details of the drive beyond H_F ; indeed, a topologically nontrivial drive can occur even if H_F acts as the identity operator in the bulk (see Ref. [26] and references therein). In the periodic table of Floquet topological insulators [27], the symmetries used in the classification relate the time-dependent Hamiltonian $H(t)$ to itself at another time, e.g., $\mathcal{C}H(t)\mathcal{C}^{-1} = -H(T_{\text{drive}} - t)$ for chiral symmetry (where T_{drive} is the driving period). We therefore propose to study, in one particular entry in the periodic table, the interplay of topology and of disorder that respects the appropriate time-dependent symmetry constraint.

The main result of this paper is a universal localization-delocalization transition for disordered, topologically nontrivial, single-particle Floquet drives in the chiral-symmetric class in one spatial dimension. We consider the time-dependent localization length $L_{\text{loc}}(t)$

* Present address: Center for Quantum Science and Engineering, Department of Electrical and Computer Engineering, University of California, Los Angeles, Los Angeles, California 90095, USA, adrianculver@g.ucla.edu

† roy@physics.ucla.edu

of a time evolution operator that represents the intrinsically dynamical part of the time evolution operator for the drive (see next paragraph), and we find that $L_{\text{loc}}(t)$ diverges with a universal exponent at a particular t within the driving period. As in the integer quantum Hall plateau transition, we have a topological obstruction to localization at a particular value of some parameter, which then leads to a localization-delocalization transition as that parameter is varied. Unlike the quantum Hall case or the one-dimensional class AIII static case (Ref. [9] mentioned above), here the parameter is time and the transition occurs throughout the (quasienergy) spectrum. Also, the transition we find does not seem to be a topological *phase* transition; see Sec. II B below for more discussion of this point.

To give a more detailed statement of our result, we recall first that any drive can be decomposed (uniquely up to homotopy) into two component drives: a static drive and an intrinsically dynamical “loop” drive $U_{\text{loop}}(t)$ ($0 \leq t \leq T_{\text{drive}}$), where the latter by definition is equal to the identity at both $t = 0$ and T_{drive} [27]. The decomposition can be done such that the loop component U_{loop} inherits the symmetries of the originally given drive, in this case chiral symmetry. Our focus is entirely on the loop component U_{loop} , which we emphasize contains the intrinsically dynamical possibilities for topology. Assuming U_{loop} to realize the simplest possibility for topological nontriviality—a value of 1 for the appropriate topological index [28]—we study the time-dependent localization length $L_{\text{loc}}(t)$ of $U_{\text{loop}}(t)$ [29]. We argue that the chiral symmetry and topological nontriviality require delocalization at the midpoint of the drive ($t = T_{\text{drive}}/2$). Since we are considering one spatial dimension, we can expect complete localization at all other times t , since there is no topological protection there. Our main claim is that there is a universal exponent for the transition that occurs as t approaches $T_{\text{drive}}/2$ from either side: $L_{\text{loc}}(t) \sim |t - T_{\text{drive}}/2|^{-\nu}$ with $\nu = 2$. The localization length generally depends on the quasienergy and on the disorder, but we claim that generically these only appear in the prefactor and not the exponent.

Our work is not directly motivated by experiment, and indeed it may be expected that both the loop decomposition and the requirement for the disorder to obey a time-dependent symmetry would present challenges to detecting the diverging localization length in a real system. One possibility for experimental realization is the close connection between Floquet drives and discrete-time quantum walks. Also, the transition we find here could serve as a theoretical toy model for other transitions.

The particular disordered Floquet drive that we use as an example for our calculations has been studied in an equivalent form in the context of discrete-time quantum walks [19, 20], as we discuss in more detail in the main text. Our claim of the universal transition for a class of drives goes beyond prior work to our knowledge. Preliminary work toward the results of this paper was reported by some of the present authors in Refs. [30, 31].

The paper is organized as follows. In Sec. II, we review the topological classification of noninteracting Floquet drives and the symmetry class AIII that is our main focus. We then state our main result, clarify the role of chiral-symmetric disorder, and discuss a possible wider scope for the universal exponent (as well as some “fine-tuned” exceptions). In Sec. III, we present analytical and numerical calculations illustrating the universal exponent in several examples of class AIII drives. In Sec. IV, we present a more general argument for the universal exponent. We conclude in Sec. V with some ideas for investigating many-body localization in class AIII drives that include interactions.

II. DISORDERED, CHIRAL-SYMMETRIC DRIVES IN ONE DIMENSION

A. Preliminary discussion

Periodically driven (Floquet) systems are described by a time-periodic Hamiltonian $\mathcal{H}(t)$ with a period T_{drive} , so that $\mathcal{H}(t + T_{\text{drive}}) = \mathcal{H}(t)$. Throughout, we consider real-space local Hamiltonians, i.e., the matrix elements in position space must be upper bounded by some decaying exponential. The unitary time evolution operator $\mathcal{U}(t)$ is given by the usual time-ordered expression $\mathcal{U}(t) = T \exp \left[-i \int_0^t dt' \mathcal{H}(t') \right]$. Note that $\mathcal{U}(t)$ need not be periodic, even though $\mathcal{H}(t)$ is.

Noninteracting Floquet topological insulators have been classified into a periodic table [27] (see Ref. [26] for a review) using the Altland–Zirnbauer symmetry classification. In particular, Floquet drives are separated into ten symmetry classes based on the presence or absence of time-reversal, particle-hole, and chiral symmetry, and the full topological classification depends on the symmetry class and the number of spatial dimensions. We focus on 1D class AIII systems, i.e., those with chiral symmetry only. This is the simplest case in which a topologically nontrivial Floquet phase can occur.

By definition, class AIII drives satisfy

$$\mathcal{C}\mathcal{H}(t)\mathcal{C}^{-1} = -\mathcal{H}(T_{\text{drive}} - t), \quad (2.1)$$

where \mathcal{C} denotes the chiral symmetry operator, which satisfies $\mathcal{C}^2 = \mathcal{C}\mathcal{C}^\dagger = \mathcal{C}^\dagger\mathcal{C} = \mathbb{1}$ and $\text{Tr } \mathcal{C} = 0$. The corresponding unitary evolution $\mathcal{U}(t)$ inherits a symmetry property (see Appendix A of Ref. [27]):

$$\mathcal{C}\mathcal{U}(t)\mathcal{C}^{-1} = \mathcal{U}(T_{\text{drive}} - t)\mathcal{U}^\dagger(T_{\text{drive}}). \quad (2.2)$$

We suppose that our Floquet drive acts on a one-dimensional lattice with basis states $|n, \alpha, s\rangle$, where n is a site index taking on integer values, $\alpha = A$ or B is a sublattice index on which the chiral symmetry acts, and s stands for any other on-site degrees of freedom. The chiral symmetry operator can be written as

$$\mathcal{C} = \tau^z, \quad (2.3)$$

where τ^z is the Pauli matrix acting on the sublattice index (and acting as the identity on the other indices).

Our focus in this work is on topological properties that are uniquely dynamical, i.e., not simply inherited from a static Hamiltonian. For this reason, we find it convenient to use the technique introduced in Ref. [27] (see also Ref. [28]) of decomposing a generic drive into a particular combination of time evolution by a static Hamiltonian and time evolution by a loop drive.

To present the loop decomposition, we first recall the definition of composition of two drives. Consider two chiral-symmetric drives $\mathcal{U}_1(t)$ and $\mathcal{U}_2(t)$ ($0 \leq t \leq T_{\text{drive}}$) which are generated by time-dependent Hamiltonians $\mathcal{H}_1(t)$ and $\mathcal{H}_2(t)$. The composition operation [27], denoted $*$, produces a new chiral-symmetric drive $\mathcal{U}(t)$ with the same period; suppressing t , we write $\mathcal{U} \equiv \mathcal{U}_1 * \mathcal{U}_2$. By definition, the drive \mathcal{U} is generated by a time-dependent Hamiltonian $\mathcal{H} \equiv \mathcal{H}_1 * \mathcal{H}_2$ given by

$$\mathcal{H}(t) = \begin{cases} 2\mathcal{H}_2(2t) & 0 \leq t < T_{\text{drive}}/4 \\ 2\mathcal{H}_1(2t - T_{\text{drive}}/2) & T_{\text{drive}}/4 \leq t \leq 3T_{\text{drive}}/4 \\ 2\mathcal{H}_2(2t - T_{\text{drive}}) & 3T_{\text{drive}}/4 < t \leq T_{\text{drive}}. \end{cases} \quad (2.4)$$

It is readily verified that $\mathcal{H}(t)$ satisfies the chiral symmetry property (2.1).

A loop drive is one that begins and ends at the identity when the system has periodic boundary conditions (or is infinite): $U_{\text{loop}}(t=0) = U_{\text{loop}}(t=T_{\text{drive}}) = 1$. A static drive is one generated by some time-independent Hamiltonian H_{static} :

$$U_{\text{static}}(t) = e^{-iH_{\text{static}}t}. \quad (2.5)$$

As shown in Ref. [27], an arbitrary chiral-symmetric drive $\mathcal{U}(t)$ is homotopic to the composition of some chiral-symmetric loop drive $U_{\text{loop}}(t)$ and some static drive $U_{\text{static}}(t)$:

$$\mathcal{U} \approx U_{\text{loop}} * U_{\text{static}}, \quad (2.6)$$

where U_{loop} and U_{static} are unique up to homotopic equivalence. We will focus on a canonical choice defined by taking $U_{\text{loop}}(t)$ to be generated by $H_{\text{loop}}(t)$ and $U_{\text{static}}(t)$ to be as in Eq. (2.5), with

$$H_{\text{loop}} = \mathcal{H} * (-H_F), \quad (2.7a)$$

$$H_{\text{static}} = H_F, \quad (2.7b)$$

where H_F is the Floquet Hamiltonian for the drive [$\mathcal{U}(T_{\text{drive}}) = e^{-iH_F T_{\text{drive}}}$]. Since our interest is in t near the midpoint, let us note here that the above equations readily yield (for $T_{\text{drive}}/4 \leq t \leq 3T_{\text{drive}}/4$)

$$U_{\text{loop}}(t) = \mathcal{U}(2t - T_{\text{drive}}/2)e^{-iH_F T_{\text{drive}}/2}. \quad (2.8)$$

We recall here that the loop decomposition requires the endpoint unitary $\mathcal{U}(T_{\text{drive}})$ to have, in the translation-invariant case, a spectral gap at quasienergy $\epsilon = \pi$. We are interested in the disordered case, so we can expect

that $\mathcal{U}(T_{\text{drive}})$ has only localized states and no spectral gap. However, the entire spectrum is then a mobility gap, and a mobility gap in particular at $\epsilon = \pi$ should suffice for doing the loop decomposition (see Refs. [27, 32]).

The decomposition (2.6) is essential to this work, as our focus throughout is on the localization properties of the loop component of the given drive $\mathcal{U}(t)$. From now on, we simplify the notation by writing the loop component as $U_{\text{loop}}(t) \equiv U(t)$.

We are interested in drives for which the loop component is topologically nontrivial. To state this condition precisely, we now review the chiral flow, the topological index introduced in Ref. [28] for the loop component of class AIII drives in one dimension. We first recall the flow index (the topological index for unitary operators without symmetry in one dimension [33]), which is used in the definition of the chiral flow.

Given a unitary matrix U acting on an infinite one-dimensional lattice, with matrix elements $U_{na,n'a'}$ (where n is the lattice site index and a labels any on-site degrees of freedom), the flow index of U is defined as

$$\nu(U) = \sum_{\substack{n \geq n_0 \\ n' < n_0}} \sum_{a,a'} (|U_{na,n'a'}|^2 - |U_{n'a',na}|^2), \quad (2.9)$$

where the site n_0 is arbitrary [and $\nu(U)$ is in fact independent of n_0]. The flow index is quantized to integer values and may be understood as the net current passing through any site n_0 . For example, the operator that translates by a certain integer has a flow index equal to that integer (e.g., the mapping $|n\rangle \rightarrow |n+1\rangle$ has a flow index of 1).

To apply the flow index to a class AIII drive, we note that the loop component of the drive inherits the same chiral symmetry property (2.2), which simplifies due to the loop property to

$$CU(t)C^{-1} = U(T_{\text{drive}} - t). \quad (2.10)$$

Due to this symmetry, the midpoint of the loop part of the drive is a special point; in particular, we have the following useful relation [28]:

$$CU(T_{\text{drive}}/2)C^{-1} = U(T_{\text{drive}}/2). \quad (2.11)$$

Recalling the form (2.3) of the chiral symmetry operator, we see that Eq. (2.11) constrains the time evolution at the midpoint to the block diagonal form

$$U(T_{\text{drive}}/2) = \begin{pmatrix} U_{AA} & 0 \\ 0 & U_{BB} \end{pmatrix}. \quad (2.12)$$

We may then consider the flow index of the two components U_{AA} and U_{BB} . Since the time evolution operator at the midpoint is generated (by assumption) by a local Hamiltonian, it follows that $\nu[U(T_{\text{drive}}/2)] = 0$ [34, 35]. From the additivity of the flow index [34], we then see that the flow indices of the two components sum to zero: $\nu(U_{AA}) + \nu(U_{BB}) = 0$. Either of the two may be taken

as the definition of the chiral flow of the loop drive $U(t)$. We follow the convention that the chiral flow is the flow index of the A component [28]:

$$\nu_{\text{chiral}}[\{U(t)\}] = \nu[U_{AA}]. \quad (2.13)$$

We are interested in topologically nontrivial drives, so we assume that the chiral flow is nonzero. More specifically, our numerics and analytical arguments focus on the case of $\nu_{\text{chiral}}[\{U(t)\}] = 1$. Let us note here that a drive with unit chiral flow can be generated by a local Hamiltonian, as shown by the explicit model introduced in Ref. [28] (and reviewed below in Sec. III); in contrast, no local Hamiltonian can generate a unitary with nonzero flow index in one dimension [34, 35].

B. Universal localization-delocalization transition

It is well-known that in one dimension, the eigenstates of a disordered, static Hamiltonian are generically localized. We can expect the same to be true for eigenstates of $U(t)$ for a generic value of the time t . However, we argue that the midpoint of the drive ($t = T_{\text{drive}}/2$) is topologically protected from localization by our assumption that the chiral flow is non-vanishing. (We do not yet make the more specific assumption that the chiral flow is equal to one.)

In particular, we present two independent arguments for the following claim: at almost any quasienergy ϵ in the spectrum of $U(T_{\text{drive}}/2)$, there must exist a delocalized eigenstate. We have checked this claim, sometimes analytically and sometimes numerically, in a variety of cases (see below). A related analysis will be presented elsewhere [36].

Due to the diagonal structure of Eq. (2.12), our claim reduces to the statement that a local unitary operator U' (which represents either U_{AA} or U_{BB}) with non-zero flow index must have delocalized states throughout its quasienergy spectrum. To sketch our first argument, we start by recalling that all U' with the same nonvanishing flow index are homotopic to a translation operator (which translates by a number of sites equal to the value of the flow index) [34]. A translation operator indeed has delocalized eigenstates throughout its spectrum, and furthermore these states are chiral, so they are perturbatively robust, similar to the edge states in a quantum Hall system.

For our second argument, we appeal to the general expectation that mobility edges are not found in one dimension. Here we ignore the known exceptions of correlated disorder and quasiperiodic systems [37] because our focus is on the generic case. Thus, it should suffice to show that U' must have a delocalized state at *some* quasienergy. To show this, we write U' in its eigenbasis:

$$U' = \sum_{\epsilon} e^{-i\epsilon T_{\text{drive}}/2} |\Psi_{\epsilon}\rangle \langle \Psi_{\epsilon}|. \quad (2.14)$$

If every eigenvector $|\Psi_{\epsilon}\rangle$ is localized, then we can take the logarithm of Eq. (2.14) to obtain a *local* Hamiltonian H_F that generates U' (via $U' = e^{-iH_F T_{\text{drive}}/2}$). But a unitary operator that is generated by a local Hamiltonian must have zero flow index [34, 35], in contradiction to our starting assumption. Thus, we conclude that some eigenvector $|\Psi_{\epsilon}\rangle$ must be delocalized (hence one expects all eigenvectors to be delocalized).

To set up the statement of our main claim, let us write the eigenstate equation for $U(t)$ explicitly:

$$U(t) |\Psi_{\epsilon}(t)\rangle = e^{-i\epsilon t} |\Psi_{\epsilon}(t)\rangle, \quad (2.15)$$

where ϵ is the quasienergy and where the t dependence in $|\Psi_{\epsilon}(t)\rangle$ is a label associating this state to $U(t)$ (*not* an indication of time evolution by the time-dependent Schrödinger equation). Since we are considering an infinitely large, disordered system, the quasienergy spectrum of $U(t)$ is gapless for all t .

Let us emphasize that we are focusing on the time evolution operator $U(t)$ with arbitrary t , not necessarily the full period ($t = T_{\text{drive}}$). One perspective on this is to consider a discrete-time process in which $U(t)$ is the operator for implementing a single time step; in other words, any given t is considered to be the full period. The properties of the eigenstates of $U(t)$ would have implications for this discrete-time process. It is in the same spirit that we use the term “quasienergy” in reference to the spectrum of $U(t)$.

We write the localization length of $|\Psi_{\epsilon}(t)\rangle$ as $L_{\text{loc}}(t)$, suppressing the dependence on ϵ . According to our arguments above, $L_{\text{loc}}(t)$ is infinite for $t = T_{\text{drive}}/2$ and finite otherwise. For a drive with $\nu_{\text{chiral}}[\{U(t)\}] = 1$, we claim that the localization length diverges with a universal exponent as t approaches the midpoint:

$$L_{\text{loc}}(t) \sim \frac{1}{(t - T_{\text{drive}}/2)^{\nu}} \quad (\nu = 2). \quad (2.16)$$

Equation (2.16) is the main claim of this paper. The constant of proportionality is non-universal and generally depends on the quasienergy; however, the exponent $\nu = 2$ holds throughout the quasienergy spectrum. We emphasize that the localization length we are considering corresponds to the instantaneous eigenstates of the loop part $U(t) \equiv U_{\text{loop}}(t)$ of the original drive.

We argue that the exponent of $\nu = 2$ is generic for loop drives in class AIII with $\nu_{\text{chiral}}[\{U(t)\}] = 1$, albeit with certain fine-tuned exceptions that we discuss below in Sec. IID.

Before presenting more detailed arguments, let us mention that there is a simple way to obtain the exponent $\nu = 2$, granting the assumption (which our calculations below support) that the Lyapunov exponent $1/L_{\text{loc}}(t)$ is an analytic function at $t = T_{\text{drive}}/2$. Due to the topological argument we discussed above, the expansion of $1/L_{\text{loc}}(t)$ about the point $t = T_{\text{drive}}/2$ can have no zeroth order term; then there can be no linear term because the Lyapunov exponent cannot be negative. Thus, this

simple argument yields the series starting generically at quadratic order, which is precisely (2.16). Our more detailed argument in Sec. IV can be roughly summarized as showing that, under some simplifying assumptions, the Lyapunov exponent is given at the leading order by a second-order polynomial in variables that start at linear order in $t - T_{\text{drive}}/2$.

Let us also comment here on the similarities and differences between our work and the integer quantum Hall effect plateau transition. In both cases, we have a varying parameter (time t or energy E) and a topological index (the chiral flow or the Chern number) that is associated with a range of values of the parameter (the driving period or the bandwidth). The eigenstates are localized at all values of the parameter except for some critical value ($T_{\text{drive}}/2$ or E_c), where delocalization must occur due to the index being nonzero. A localization-delocalization transition therefore occurs as the parameter crosses the critical value. One crucial difference is that the quantum Hall case has a topological phase transition, while our case, as far as we know, does not. The quantum Hall case is a static problem, so a topological phase can be defined by the index of the ground state, and thus a topological phase transition occurs as the Fermi energy crosses E_c (since the extended state carries the Chern number). In a Floquet problem, though, it is not clear what could play the role of the ground state or Fermi energy. Another difference is that there is a noninteger delocalization exponent in the quantum Hall case (in particular, the Lyapunov exponent is nonanalytic at $E = E_c$); in our case, we have a scattering argument that yields analyticity at $t = T_{\text{drive}}/2$ and thus an integer exponent.

C. Chiral-symmetric disorder in loop drives

In this section, we clarify the role of disorder in our setup. Our main claim (2.16) is meant to apply to any *particular* drive, i.e., the thermodynamic limit of a single disorder realization (as long as the realization is suitably generic). For calculations, we find it convenient to use the idea of self-averaging from the theory of disordered systems, which refers to the fact that for appropriately chosen physical quantities, the relative fluctuations over an ensemble of disorder realizations vanish in the thermodynamic limit. For these quantities, the value in any particular system can also be obtained by averaging over an ensemble of disorder realizations. Note that the lo-

calization length that we have discussed above is really the thermodynamic limit of a size-dependent localization length and furthermore, this quantity may be expected to be self-averaging.

Our basic assumption is that the given drive $\mathcal{U}(t)$ is in some sense a disordering of an underlying translationally invariant (“clean”) drive $\mathcal{U}_{\text{clean}}(t)$. According to self-averaging, we could determine properties of a particular, generic $\mathcal{U}(t)$ by averaging over an ensemble of disorder realizations (each chiral-symmetric) of $\mathcal{U}_{\text{clean}}(t)$; however, this is inconvenient for calculations because we would then need to do the decomposition (2.6) on each member of the ensemble.

We instead proceed as follows: we do the decomposition (2.6) on $\mathcal{U}(t)$ and on $\mathcal{U}_{\text{clean}}(t)$ to yield loop drives $U(t)$ and $U_{\text{clean}}(t)$, respectively. We then regard $U(t)$, which is a particular drive, as a member of an ensemble of disorderings of $U_{\text{clean}}(t)$. Each member of the ensemble is a chiral-symmetric loop drive. By considering a range of possible disorder distributions in such an ensemble, we expect that properties of a generic starting drive $\mathcal{U}(t)$ are being probed.

We now present, for use in our subsequent calculations in specific example models, one particular way of adding disorder to a given translationally invariant, chiral-symmetric loop drive $U_{\text{clean}}(t)$. We provide this construction because it is not immediately obvious how to include disorder that respects the required properties, even if one is given the explicit Hamiltonian $H_{\text{clean}}(t)$ that generates $U_{\text{clean}}(t)$; disordering the parameters of $H_{\text{clean}}(t)$ generally results in a drive that fails to satisfy the chiral symmetry requirement, the loop condition, or both. After presenting this particular construction for including disorder, we discuss some general properties of a disordered drive that hold regardless of the precise way the disorder is included.

Our construction takes as given, in addition to the chiral-symmetric Hamiltonian $H_{\text{clean}}(t)$ with period T_{drive} that generates $U_{\text{clean}}(t)$, a static disordered Hamiltonian H_d that commutes with the chiral symmetry operator:

$$\mathcal{C}^{-1}H_d\mathcal{C} = H_d. \quad (2.17)$$

Note that this condition is equivalent to H_d being block diagonal in the A-B basis. We further assume that $H_d \rightarrow 0$ in the limit of no disorder.

We choose an arbitrary constant time $T_0 > 0$ and define a new drive $H(t)$ with a period of $T_{\text{drive}} + T_0$:

$$H(t) = \begin{cases} H_d & 0 < t < T_0/2 \\ H_{\text{clean}}(t - T_0/2) & T_0/2 \leq t \leq T_{\text{drive}} + T_0/2 \\ -H_d & T_0/2 + T_{\text{drive}} < t \leq T_{\text{drive}} + T_0, \end{cases} \quad (2.18)$$

with $H(t + T_{\text{drive}} + T_0) = H(t)$. The time evolution operator from $t = 0$ to any $t \in [0, T_{\text{drive}} + T_0]$, expressed in terms

of $U_{\text{clean}}(t)$ and H_d , is

$$U(t) \equiv T \exp \left(-i \int_0^t dt' H(t') \right) \quad (2.19a)$$

$$= \begin{cases} e^{-iH_d t} & 0 < t < T_0/2 \\ U_{\text{clean}}(t - T_0/2) e^{-iH_d T_0/2} & T_0/2 \leq t \leq T_0/2 + T_{\text{drive}} \\ e^{iH_d(t - T_{\text{drive}} - T_0)} & T_0/2 + T_{\text{drive}} < t \leq T_{\text{drive}} + T_0, \end{cases} \quad (2.19b)$$

where we have used the loop condition $U_{\text{clean}}(T_{\text{drive}}) = 1$. It is readily verified that $U(t)$ is a chiral-symmetric loop drive; in particular, $H(t)$ satisfies (2.1) (with the period increased from T_{drive} to $T_{\text{drive}} + T_0$) and $U(T_{\text{drive}} + T_0) = 1$.

For convenience, we now take a limit so the disordered drive has the same period as the clean drive. To do this, we send $T_0 \rightarrow 0$ with H_d scaling with T_0 in such a way that $H_d T_0$ remains fixed. We thus obtain a disordered unitary operator

$$U_d = \lim_{\substack{T_0 \rightarrow 0 \\ H_d T_0 \text{ fixed}}} e^{-iH_d T_0/2}, \quad (2.20)$$

and we may write the disordered drive with a period of T_{drive} :

$$U(t) = U_{\text{clean}}(t) U_d \quad (0 \leq t < T_{\text{drive}}). \quad (2.21)$$

Equation (2.21) is to be understood as shorthand for the limit of Eq. (2.19b). In particular, it is understood that if t is set exactly to T_{drive} , then an additional factor of U_d^\dagger appears multiplying $U_{\text{clean}}(T_{\text{drive}}) = 1$ on the left, which restores the loop condition [$U(T_{\text{drive}}) = 1$]. Then the chiral symmetry relation (2.1) holds due to $\mathcal{C} U_d \mathcal{C}^{-1} = U_d$, which follows from the assumption that H_d commutes with \mathcal{C} .

We next present an alternate approach in which the disordered drive is not explicitly constructed, but instead expanded about the midpoint of the drive (which is the regime of interest for the universal exponent). This approach clarifies the assumption we make that the drive is generic; indeed, we show that if a certain fine-tuned condition is satisfied, then the localization length may diverge with an exponent greater than 2.

A general drive may be expanded about the midpoint ($t = T_{\text{drive}}/2$) in powers of Δt :

$$U(T_{\text{drive}}/2 + \Delta t) = [1 - iH(T_{\text{drive}}/2)\Delta t + O((\Delta t)^2)] \times U(T_{\text{drive}}/2). \quad (2.22)$$

If $H(t)$ is piecewise smooth with a discontinuity at $T_{\text{drive}}/2$, then $H(T_{\text{drive}}/2)$ here is replaced by its right (left) limit as $t \rightarrow T_{\text{drive}}/2$ when Δt is positive (negative).

The expansion (2.22) provides an alternate way to probe the ensemble of allowed disorderings of a given translation-invariant loop drive $U_{\text{clean}}(t)$. The disordered

drive $U(t)$ must at least respect the chiral symmetry and the loop property, in addition to reducing to $U_{\text{clean}}(t)$ in the absence of disorder. It may be difficult to find explicit examples [aside from the construction (2.21) that we have already provided] of $U(t)$ that satisfy these properties; however, we know that *any* valid $U(t)$ has some $U(T_{\text{drive}}/2)$ and $H(T_{\text{drive}}/2)$ [with $U(T_{\text{drive}}/2)$ satisfying the symmetry relation (2.11)], which reduce to the corresponding terms for $U_{\text{clean}}(t)$ in the absence of disorder. We expect, then, that for t near the midpoint, we can probe the ensemble of allowed disorderings of the drive $U_{\text{clean}}(t)$ by specifying various disordered operators that act on the same Hilbert space as $U_{\text{clean}}(t)$ and then assuming these operators to be $U(T_{\text{drive}}/2)$ and $H(T_{\text{drive}}/2)$ of some $U(t)$. We can then use the expansion (2.22) without knowing the full form of $U(t)$.

We do not pursue the problem of completing the drive, i.e., constructing a chiral-symmetric loop drive $U(t)$ for all t that recovers the given $U(T_{\text{drive}}/2)$ and $H(T_{\text{drive}}/2)$. However, we expect that some chiral-symmetric loop drive completion can always be found.

D. Exceptions to the universal exponent, and further generality

Here we identify a necessary condition for the exponent to be $\nu = 2$. We argue that this condition should hold for a generic drive (with possible fine-tuned exceptions). This discussion naturally leads us to a wider setting, not necessarily connected to chiral-symmetric drives, in which we claim that our main result (2.16) holds.

Note first that we can decompose any operator \mathcal{O} into parts that commute and anticommute with the chiral symmetry operator:

$$\mathcal{O} = \mathcal{O}_- + \mathcal{O}_+, \quad (2.23)$$

where $[\mathcal{O}_-, \mathcal{C}] = \{\mathcal{O}_+, \mathcal{C}\} = 0$. Applying this to $\mathcal{O} = H(t)$, we see that the anticommuting part of the chiral symmetry equation (2.1) for $t = T_{\text{drive}}/2 + \Delta t$ yields

$$H_+(T_{\text{drive}}/2 + \Delta t) = H_+(T_{\text{drive}}/2 - \Delta t), \quad (2.24)$$

where Δt is arbitrary. In particular, $H_+(t)$ is continuous at $t = T_{\text{drive}}/2$, so we can consider $H_+(T_{\text{drive}}/2)$ without needing to distinguish the left and right limits.

We will assume, as part of the definition of a drive being generic, that the anticommuting part of the Hamiltonian at the midpoint is nonvanishing:

$$H_+(T_{\text{drive}}/2) \neq 0. \quad (2.25)$$

Note that there is no symmetry that requires this term to vanish. If instead $H_+(T_{\text{drive}}/2) = 0$, then the Δt correction term in the expansion (2.22) commutes with \mathcal{C} ; then, $U(T_{\text{drive}}/2 + \Delta t)$ remains block-diagonal in the A - B basis up to corrections of order $(\Delta t)^2$. The block-diagonal structure preserves the topological protection to another order, and hence the localization length exponent ν can be larger than 2 in this case.

More generally, we expect the exponent $\nu = 2$ to hold whenever we have a family of drives that can be expanded in the form of Eq. (2.22). In particular, let \tilde{U} be any local unitary operator (not drive) that takes the block-diagonal form of (2.12) in some basis. Suppose that the flow indices of the diagonal components satisfy $\nu(U_{AA}) = -\nu(U_{BB}) = 1$. Consider the family of time evolutions defined by

$$\tilde{U}(\Delta t) = T \exp \left[-i \int_0^{\Delta t} dt' H(t') \right] U_0, \quad (2.26)$$

where $\tilde{H}(t)$ is some local Hamiltonian with no symmetries assumed. Then we have the following expansion for small Δt :

$$\tilde{U}(\Delta t) = [1 - iH(\Delta t = 0)\Delta t + O((\Delta t)^2)] \tilde{U}_0. \quad (2.27)$$

We claim that the localization length L_{loc} of $\tilde{U}(\Delta t)$ follows the same exponent (2.16) provided that the condition analogous to (2.25) holds, i.e.,

$$\{H(\Delta t = 0), \tau^z\} \neq 0, \quad (2.28)$$

where τ^z is the Pauli matrix acting on the space in which \tilde{U}_0 is block diagonal.

III. EXAMPLE DRIVES WITH THE UNIVERSAL EXPONENT

We now provide several example class AIII drives in which we find that the delocalization exponent is 2. The starting point in these examples is a clean drive previously introduced in Ref. [28]. With on-site disorder included, we demonstrate rigorously that the exponent is $\nu = 2$ by using a result from the mathematics literature on products of random matrices [38]. In the special case of full phase disorder, we obtain an analytical result for the localization length at any time t in the drive, which agrees with results found in similar models that have been studied in the context of discrete-time quantum walks. We then allow disorder that couples neighboring sites within dimers, and we find that our prediction of $\nu = 2$ is consistent with transfer matrix numerics.

Finally, we introduce disorder with exponential decay in position space, and we find that our prediction of $\nu = 2$ is consistent with exact diagonalization numerics. For further numerical checks, see Ref. [30].

We begin by recalling the drive introduced in Ref. [28]. The model is a Floquet version of the Su-Schrieffer-Heeger (SSH) model [39], and will be referred to hereafter as the SSH-type drive. The drive occurs on an infinite one-dimensional bipartite lattice with sublattice degrees of freedom labeled A and B . The drive consists of piecewise-constant evolution by two Hamiltonians: H_1 , which is an SSH Hamiltonian in the trivial phase, and H_2 , which is an SSH Hamiltonian in the topological phase. In particular, we define

$$H_1 = \frac{2\pi}{T_{\text{drive}}} \sum_n (|n, A\rangle \langle n, B| + \text{H.c.}), \quad (3.1a)$$

$$H_2 = -\frac{2\pi}{T_{\text{drive}}} \sum_n (|n+1, A\rangle \langle n, B| + \text{H.c.}), \quad (3.1b)$$

where n is the site index and T_{drive} is the period of the drive. The time-dependent Hamiltonian is given by

$$H(t) = \begin{cases} H_1 & 0 \leq t < \frac{T_{\text{drive}}}{4} \\ H_2 & \frac{T_{\text{drive}}}{4} \leq t \leq \frac{3T_{\text{drive}}}{4} \\ H_1 & \frac{3T_{\text{drive}}}{4} < t \leq T_{\text{drive}}. \end{cases} \quad (3.2)$$

The time evolution operator for the drive is then given by the usual expression $U_{\text{clean}}(t) = T \exp \left[-i \int_0^t dt' H(t') \right]$. As discussed in Ref. [28], the one-dimensional AIII topological index (the chiral flow) for this drive is equal to 1. This can be seen by noting that the time evolution operator at $t = T_{\text{drive}}/2$ acts separately on the A and B sublattices, and is given by

$$U_{\text{clean}}(t = T_{\text{drive}}/2) = \begin{pmatrix} \hat{T}_A & 0 \\ 0 & \hat{T}_B^\dagger \end{pmatrix}, \quad (3.3)$$

where \hat{T}_α ($\alpha = A, B$) translates the corresponding sublattice by one unit cell to the right. Thus, the effect of the time evolution operator at the midpoint of the drive is the translation of all the A orbital amplitudes by one unit cell to the right, and the translation of all the B orbital amplitudes by one unit cell to the left.

The quasienergy spectrum of $U_{\text{clean}}(t)$ is gapless at $t = T_{\text{drive}}/2$ and gapped elsewhere (Fig. 1). We present the explicit calculation in Appendix A 2 for completeness. Alternatively, we can read off the solution by noting that the eigenstate problem for $U(t)$ [Eq. (2.15)] is equivalent to a type of discrete-time quantum walk considered in Ref. [19]. Our parameter Δt corresponds to the coin parameter of the quantum walk (see Appendix A 1 for details).

We note here that if the model is considered with open boundary conditions [by restricting the sums over n to $1, \dots, N$ in Eq. (3.1a) and $1, \dots, N-1$ in Eq. (3.1b)], then the time evolution operator for a full period acts as

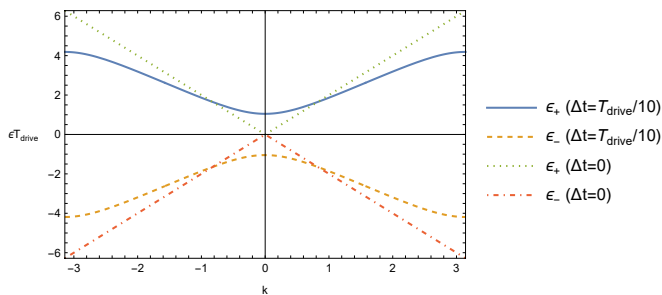


FIG. 1: The two quasienergy bands $\epsilon_{\pm}(k)$ of the clean SSH-type drive. For any $|\Delta t| < T_{\text{drive}}/4$, there is a gap, except at the midpoint of the drive ($\Delta t = 0$, $\epsilon_{\pm}(k) = \pm 2|k|/T_{\text{drive}}$). Here we have included the dimensional factor T_{drive} that we usually set to 2π .

the identity in the bulk but not at the edges. Indeed, sites at the edges (B at $n = 1$ and A at $n = N$) gain a phase of π under evolution by a full period [28]. This micromotion at the edges is similar to the anomalous edge transport that occurs in the Rudner-Lindner-Berg-Levin model in two spatial dimensions [40].

In accordance with the general arguments of Sec. II B, we find that for a variety of disorderings of this drive, the localization length follows the behavior (2.16). Let us note here that the localization length can be defined in various ways depending on the boundary conditions imposed on the model; the different definitions can be expected to become equivalent in the thermodynamic limit. We present explicit definitions below.

Throughout the calculations below, we set $T_{\text{drive}} = 2\pi$ for convenience. We write an eigenstate $|\Psi_{\epsilon}(t)\rangle$ of $U(t)$ [c.f. Eq. (2.15)] as

$$|\Psi_{\epsilon}(t)\rangle = \sum_n (\Psi_{n,A} |n, A\rangle + \Psi_{n,B} |n, B\rangle), \quad (3.4)$$

suppressing the ϵ and t dependence of $\Psi_{n,A}$ and $\Psi_{n,B}$, and we define

$$\Psi_n = \begin{pmatrix} \Psi_{n,A} \\ \Psi_{n,B} \end{pmatrix}. \quad (3.5)$$

A. On-site disorder

1. Setup

We introduce two types of disorder into the SSH-type drive: phase disorder and bond disorder. In the case of phase disorder only, we construct a disordered loop drive $U(t)$ using the approach described above Eq. (2.21). As we see below, phase disorder amounts to including a disordered Hamiltonian H_d with random on-site energies. In

the case of bond disorder (possibly allowing both bond and phase disorder), we follow the approach described by Eq. (2.22) and the discussion below there, in which we do not explicitly construct the full loop drive, but instead expand about the midpoint. Bond disorder may loosely be thought of as disorder in the hopping amplitudes of the topologically nontrivial Hamiltonian H_2 in Eq. (3.1b).

To introduce phase disorder, we construct a disordered unitary operator U_d and consider the drive $U(t)$ defined by Eq. (2.21). The disordered unitary is

$$U_d = \sum_n (e^{i\phi_{n,A}} |n, A\rangle \langle n, A| + e^{i\phi_{n,B}} |n, B\rangle \langle n, B|), \quad (3.6)$$

where $\phi_{n,A}$ and $\phi_{n,B}$ are disordered phases. In particular, we will assume that $\phi_{n,A}$ and $\phi_{n,B}$ are each independently and identically distributed (i.i.d.), with disorder distributions (one for the A phases and another for the B phases) that we need not specify at this point.

Let us verify that U_d satisfies the required properties. To do this, we must find a Hamiltonian H_d that commutes with the chiral operator \mathcal{C} and that yields U_d through Eq. (2.20). We take H_d to consist of disordered on-site energies:

$$H_d = \frac{2}{T_0} \sum_n (\phi_{n,A} |n, A\rangle \langle n, A| + \phi_{n,B} |n, B\rangle \langle n, B|). \quad (3.7)$$

Then it is clear that H_d commutes with \mathcal{C} and that Eq. (2.20) holds.

It is straightforward to show that the eigenstate equation (2.15) is equivalent to [30]

$$e^{-i\epsilon t} \Psi_{n,A} = \cos(\Delta t) e^{i\phi_{n-1,A}} \Psi_{n-1,A} + i \sin(\Delta t) e^{i\phi_{n,B}} \Psi_{n,B}, \quad (3.8a)$$

$$e^{-i\epsilon t} \Psi_{n,B} = i \sin(\Delta t) e^{i\phi_{n,A}} \Psi_{n,A} + \cos(\Delta t) e^{i\phi_{n+1,B}} \Psi_{n+1,B}. \quad (3.8b)$$

This completes the setup of the SSH-type drive with phase disorder. In this case, we have explicitly constructed a disordered, chiral-symmetric loop drive that can be studied at any t in the driving period, though our main focus is on the regime of $t \approx T_{\text{drive}}/2$.

To include bond disorder, we do not explicitly construct the full loop drive for all t , but instead expand about the midpoint $t = T_{\text{drive}}/2$ [see Eq. (2.22)]. We take $U(T_{\text{drive}}/2)$ and $H(T_{\text{drive}}/2)$ as given disordered operators. We consider $U(T_{\text{drive}}/2)$ to be as in the clean SSH-type drive with phase disorder and $H(T_{\text{drive}}/2)$ to be H_2 from the SSH-type drive with disorder in the hopping amplitudes; that is,

$$U(T_{\text{drive}}/2) = \sum_n (|n+1, A\rangle \langle n, A| + |n-1, B\rangle \langle n, B|) U_d, \quad (3.9a)$$

$$H(T_{\text{drive}}/2) = - \sum_n v_n (|n+1, A\rangle \langle n, B| + \text{H.c.}), \quad (3.9b)$$

where U_d is given by Eq. (3.6) and where the v_n variables are i.i.d. with some distribution.

By a straightforward calculation, we find that the eigenstate equation (2.15) is equivalent to

$$e^{-i\epsilon t} \Psi_{n,A} = e^{i\phi_{n-1,A}} \Psi_{n-1,A} + ie^{i\phi_{n,B}} v_{n-1} \Delta t \Psi_{n,B} + O((\Delta t)^2), \quad (3.10a)$$

$$e^{-i\epsilon t} \Psi_{n,B} = ie^{i\phi_{n,A}} v_n \Delta t \Psi_{n,A} + e^{i\phi_{n+1,B}} \Psi_{n+1,B} + O((\Delta t)^2). \quad (3.10b)$$

This completes the setup of the combination of bond and phase disorder in the approach of expanding about the midpoint.

We next consider a more general problem that can be specialized to either of the two setups above. In particu-

lar, we consider the state determined by

$$e^{-i\epsilon t} \Psi_{n,A} = e^{i\phi_{n-1,A}} \cos(v_{n-1} \Delta t) \Psi_{n-1,A} + ie^{i\phi_{n,B}} \sin(v_{n-1} \Delta t) \Psi_{n,B}, \quad (3.11a)$$

$$e^{-i\epsilon t} \Psi_{n,B} = ie^{i\phi_{n,A}} \sin(v_n \Delta t) \Psi_{n,A} + e^{i\phi_{n+1,B}} \cos(v_n \Delta t) \Psi_{n+1,B}. \quad (3.11b)$$

By studying Eqs. (3.11a) and (3.11b), we can simultaneously consider both the case of phase disorder (on a disordered loop drive defined for all Δt) and the case of a combination of phase and bond disorder (defined explicitly only for small Δt). To see this, we note that setting all $v_n = 1$ recovers Eqs. (3.8a) and (3.8b), while expanding in Δt recovers Eqs. (3.10a) and (3.10b).

Equations (3.11a) and (3.11b) may be brought to the following transfer matrix form:

$$\Psi_{n+1} = \mathcal{M}_n \Psi_n, \quad (3.12)$$

where the transfer matrix is

$$\mathcal{M}_n = \begin{pmatrix} e^{i(\epsilon t + \phi_{n,A})} \sec(v_n \Delta t) & i \tan(v_n \Delta t) \\ -ie^{i(\phi_{n,A} - \phi_{n+1,B})} \tan(v_n \Delta t) & e^{-i(\epsilon t + \phi_{n+1,B})} \sec(v_n \Delta t) \end{pmatrix}. \quad (3.13)$$

Using the mapping to discrete-time quantum walks that we present in Appendix A1, we can show that the transfer matrix (3.13) is a special case of a transfer matrix obtained in Ref. [19]. Note that, although a 4×4 transfer matrix might have been expected (since we have a bipartite lattice with nearest-neighbor coupling), there is in fact a 2×2 transfer matrix [19]. For the case of phase disorder only, Eq. (3.13) was also obtained by some of the present authors in Ref. [30].

2. Localization length—calculation in position space

For our first calculation of the localization length for the problem specified by Eqs. (3.11a) and (3.11b), we use a position space approach. The time-dependent Lyapunov

exponent $\gamma(t)$ is defined by

$$\gamma(t) = \lim_{N \rightarrow \infty} \frac{1}{N} \langle \ln \|\mathcal{M}_N \dots \mathcal{M}_1\| \rangle_{1\dots N}, \quad (3.14)$$

where the double brackets indicate a matrix norm (e.g., the 2-norm) and the subscripts $1, \dots, N$ indicate the average over all disorder variables associated with those sites ($\phi_{1,A}, \dots, \phi_{N,A}$, etc.). The localization length and Lyapunov exponent are related by $1/L_{\text{loc}}(t) = \gamma(t)$.

Products of random matrices have been extensively studied in the mathematics literature. In particular, a result by Schrader *et al.* in Ref. [38] can be applied to our present problem to yield the Lyapunov exponent to the leading order in Δt . The final result is (see Appendix A3a for details)

$$\frac{1}{L_{\text{loc}}(t)} = \frac{1}{2} \left(\langle v_n^2 \rangle_n + 2\text{Re} \left[\frac{\langle v_n \rangle_n^2 \langle e^{i\phi_{n,A}} \rangle_n \langle e^{i\phi_{n,B}} \rangle_n}{e^{-2\pi i \epsilon} - \langle e^{i\phi_{n,A}} \rangle_n \langle e^{i\phi_{n,B}} \rangle_n} \right] \right) (\Delta t)^2 + O((\Delta t)^3), \quad (3.15)$$

where n is any site and $\langle \dots \rangle_n$ indicates the average over the disorder variables of that site ($\phi_{n,A}$, $\phi_{n,B}$, and v_n). Note that the leading term is proportional to $(\Delta t)^2$. This demonstrates that for the SSH-type drive with the on-site disorder that we have considered in this section, our main claim [Eq. (2.16)] holds.

B. Phase disorder in dimers

As a further probe of the universality of the localization length exponent, we introduce a type of phase disorder into the SSH-type drive that extends beyond individual sites. We group adjacent sites $(2n-1, 2n)$ (for any integer n) into dimers and introduce phase disorder that couples the two sites within each dimer. We find that this drive may be described by a 2×2 transfer matrix. We then study this transfer matrix numerically and show that the localization length has an exponent consistent with $\nu = 2$.

We introduce dimer phase disorder as a natural generalization of the on-site phase disorder considered in Sec. III A. In particular, we allow the disordered Hamiltonian H_d to include both on-site terms and terms that couple sites within the same dimer (i.e., the sites $2n-1$ and $2n$). For H_d to commute with the chiral symmetry operator, as is required for the construction of Sec. II C, the A amplitudes must not be coupled with the B amplitudes. The most general such H_d acts as some Hermitian matrix on each pair $|2n-1, A\rangle$ and $|2n, A\rangle$, and as another Hermitian matrix on each pair $|2n-1, B\rangle$ and $|2n, B\rangle$. The disordered unitary operator $U_d = e^{-iH_d T_0/2}$ then acts as some unitary matrix $U_{n,A}$ on each pair $|2n-1, A\rangle$ and $|2n, A\rangle$, and as another unitary matrix $U_{n,B}$ on each pair $|2n-1, B\rangle$ and $|2n, B\rangle$.

We find it more convenient to formulate the problem in terms of the matrix elements of $U_{n,A}$ and $U_{n,B}$, rather than in terms of the parameters of H_d that generate these matrices. Parametrizing the disordered unitary matrices as

$$U_{n,\alpha} = \begin{pmatrix} U_{n,\alpha}^{(1,1)} & U_{n,\alpha}^{(1,2)} \\ U_{n,\alpha}^{(2,1)} & U_{n,\alpha}^{(2,2)} \end{pmatrix} \quad (\alpha = A \text{ or } B), \quad (3.16)$$

we then write disordered unitary operators for each dimer as

$$\mathcal{U}_{n,\alpha} = \sum_{j,m=1,2} |2n-2+j, \alpha\rangle \langle 2n-2+m, \alpha| U_{n,\alpha}^{(j,m)}, \quad (3.17)$$

where $\alpha = A$ or B . The disordered unitary is then a sum over the dimers:

$$U_d = \sum_n (\mathcal{U}_{n,A} + \mathcal{U}_{n,B}). \quad (3.18)$$

We do not yet specify the disorder distribution but will assume that $U_{n,A}$ and $U_{n,B}$ separately are i.i.d. across the dimers labeled by n .

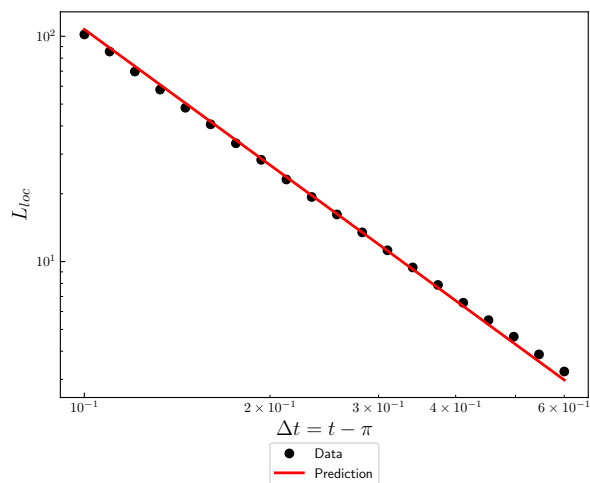


FIG. 2: The localization length in the SSH-type drive with the dimer disorder described in Sec. III B. The disordered matrices $U_{n,A}$ and $U_{n,B}$ were chosen uniformly from $U(2)$ using the Haar measure. The localization length at quasienergy ϵ is calculated according to $L_{\text{loc}}(t) = \gamma(t)^{-1}$, wherein $\gamma(t)$ is the Lyapunov exponent defined in Eq. (3.14), with the matrix norm chosen to be the spectral norm. The localization length at each value of Δt is computed for $\epsilon = 0.1$ using $L = 10^6$ transfer matrices. The prediction curve is a linear fit assuming $\nu = 2$ [i.e., $1/L_{\text{loc}}(t) = c(\Delta t)^2$ with fit parameter c].

Then, Eq. (2.21) defines a chiral-symmetric loop drive $U(t)$ with phase disorder within each dimer, generalizing the on-site case considered in the previous section. We now set up the transfer matrix to do numerical calculations of the localization length. As the calculation is lengthy, we defer details to the Appendix and summarize the result as follows. The eigenstate equation for the drive [Eq. (2.15)] may be written equivalently as a transfer matrix equation involving two of the four amplitudes in adjacent dimers, and a second equation that relates the amplitudes within one dimer:

$$\begin{pmatrix} \Psi_{2n+1,A} \\ \Psi_{2n+2,B} \end{pmatrix} = \mathcal{M}_{n,\text{dimer}} \begin{pmatrix} \Psi_{2n-1,A} \\ \Psi_{2n,B} \end{pmatrix}, \quad (3.19a)$$

$$\begin{pmatrix} \Psi_{2n-1,B} \\ \Psi_{2n,A} \end{pmatrix} = \mathcal{M}'_{n,\text{dimer}} \begin{pmatrix} \Psi_{2n-1,A} \\ \Psi_{2n,B} \end{pmatrix}. \quad (3.19b)$$

The transfer matrix $\mathcal{M}_{n,\text{dimer}}$ is a function of $U_{n,A}$, $U_{n+1,A}$, $U_{n,B}$, $U_{n+1,B}$, ϵ , and t (see Appendix B for the explicit expression), and the Lyapunov exponent $\gamma(t)$ is given by Eq. (3.14) with \mathcal{M}_n replaced by $\mathcal{M}_{n,\text{dimer}}$. The explicit form of the other matrix ($\mathcal{M}'_{n,\text{dimer}}$) is not needed.

We have thus brought the problem to a transfer matrix form, which is convenient for numerics. We calculate the Lyapunov exponent numerically at several values of Δt , with results consistent with our prediction of $\nu = 2$ (see Fig. 2). It does not seem feasible, though, to obtain an

analytical answer using the result from Ref. [38], because this result requires the disorder to separate across the transfer matrices, whereas here the disordered matrices $U_{n,A}$ and $U_{n,B}$ appear in both $\mathcal{M}_{n,\text{dimer}}$ and $\mathcal{M}_{n-1,\text{dimer}}$.

C. Longer-range disorder

As a further test of the universality of the exponent $\nu = 2$, we do a numerical test using a version of disorder that extends beyond dimers. In particular, we consider disorder that decays exponentially in real space. Due to this longer range, we cannot set up a transfer matrix calculation. We therefore impose periodic boundary conditions and use exact diagonalization to calculate the localization length numerically (see below).

We again define a disordered drive by Eqs. (2.20) and (2.21), this time using a disordered Hamiltonian H_d that couples nearest neighbors. In particular, we take H_d to be an independent copy of the static Anderson model (nearest-neighbor hopping with disordered on-site energies) on each sublattice:

$$H_d = \sum_{n,\alpha} \epsilon_{n\alpha} |n, \alpha\rangle \langle n, \alpha| - V \sum_{n,\alpha} (|n+1, \alpha\rangle \langle n, \alpha| + \text{H.c.}). \quad (3.20)$$

Since the two sublattices are decoupled, we have the required condition that H_d commutes with the chiral symmetry. Although H_d only couples nearest neighbors, U_d extends farther because it is obtained by exponentiating H_d . (In fact, it can be shown that U_d must be exponentially local in real space [32].)

From Eq. (2.20), we see that the dimensionless quantities that appear in U_d are $\epsilon_{n\alpha} T_0$ and VT_0 . We consider uniform on-site disorder; in particular, we take $\epsilon_{n\alpha} T_0/2$ to be uniformly distributed (independently on each site and sublattice) in $[-\pi, \pi]$. We also set $VT_0/2 = 1$. To reduce numerical noise, we average the localization length over all quasienergies. Due to this averaging, we are testing a weaker version of (2.16). The numerical results are consistent with the exponent $\nu = 2$ (Fig. 3).

The numerical calculation of the localization length is done as follows. At a given value of t , we consider a sequence of system sizes L . At each L , we use exact diagonalization to find all eigenstates of $U(t)$. The L -dependent localization length $L_{\text{loc}}(t, L)$ of each eigenstate $|\Psi_\epsilon(t)\rangle$ is defined as the root-mean-square variation in position space:

$$L_{\text{loc}}(t, L) = \sqrt{\langle |\Psi_\epsilon(t)\rangle | (\hat{X} - \bar{X})^2 | \Psi_\epsilon(t)\rangle}, \quad (3.21)$$

where \hat{X} is the position operator:

$$\hat{X} = \sum_{n=1}^L \sum_{\alpha=A,B} n |n, \alpha\rangle \langle n, \alpha|, \quad (3.22)$$

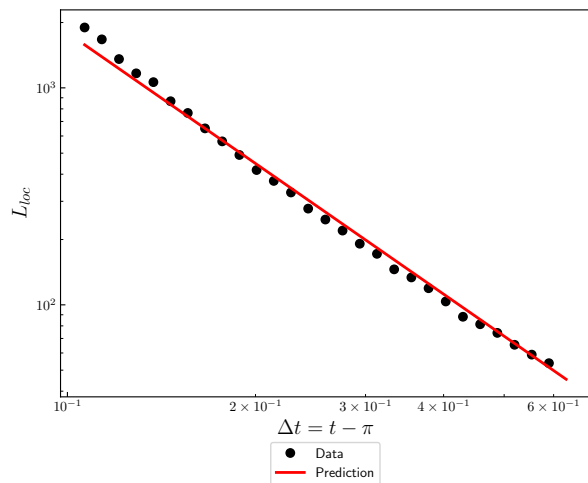


FIG. 3: Test of the universal exponent in the SSH-type drive with the longer-range disorder obtained from Eq. (3.20). The prediction curve is a linear fit assuming $\nu = 2$ [i.e., $1/L_{\text{loc}}(t) = c(\Delta t)^2$ with fit parameter c].

and where the mean value \bar{X} is defined in the appropriate way for periodic boundary conditions [41]:

$$\bar{X} = \frac{L}{2\pi} \text{Im} \left[\ln \langle \Psi_\epsilon(t) | e^{2\pi i \hat{X}/L} | \Psi_\epsilon(t) \rangle \right]. \quad (3.23)$$

We are interested in the localization length in the thermodynamic limit, that is, $L_{\text{loc}}(t) \equiv \lim_{L \rightarrow \infty} L_{\text{loc}}(t, L)$. To calculate this, we fit the L -dependent data to $L_{\text{loc}}(t, L) = L_{\text{loc}}(t) - ae^{-bL}$ with fit parameters $L_{\text{loc}}(t)$, a , and b . (For smaller values of L , we also average over multiple disorder realizations.) This procedure is done for each eigenstate, and the average of $L_{\text{loc}}(t, \epsilon)$ over all eigenstates yields a data point in Fig. 3.

IV. SCATTERING ARGUMENT FOR THE UNIVERSAL EXPONENT

In the thermodynamic limit, it can be expected that the localization length should not depend on the choice of boundary conditions. We find that scattering boundary conditions (defined below) are convenient for making an analytical argument for the universality of the exponent $\nu = 2$.

To set up the scattering problem, we write the time-dependent Hamiltonians that generate the drives $U(t)$ and $U_{\text{clean}}(t)$ as $H(t)$ and $H_{\text{clean}}(t)$, respectively. We assume that the disorder in $H(t)$ is short-range correlated, in the following sense: We have

$$H(t) = H_{\text{clean}}(t) + H_{\text{disorder}}(t), \quad (4.1)$$

where

$$H_{\text{disorder}}(t) = \sum_n \Theta_n(t), \quad (4.2)$$

and each operator $\Theta_n(t)$ is exponentially localized near the site n . Furthermore, the decay lengths are upper bounded by a number that is constant in the thermodynamic limit and independent of t .

We then define a disordered “sample,” consisting of the sites $n = 1, \dots, N$, by setting $\Theta_n(t) = 0$ for all $n \leq 0$ and $n \geq N + 1$. The $\Theta_n(t)$ operators in the sample are i.i.d. with some probability distribution. The infinite regions to the right and left of the sample are the “leads.” Although the matrix elements of the corresponding unitaries, $U(t)$ and $U_{\text{clean}}(t)$, need not be exactly equal, they can be expected to be asymptotically equal: $U_{nn'}(t) \rightarrow U_{\text{clean},nn'}(t)$ far from the disordered region (with error exponentially suppressed in the distance). This permits a scattering treatment for the eigenstate wavefunctions of $U(t)$.

Let us pause here for a technical point. It would be more natural to take the disorder to be of the form of Eq. (4.2) for the Hamiltonian $\mathcal{H}(t)$ that generates the original drive $U(t)$, rather than for the Hamiltonian $H(t)$ that generates the loop drive $U(t)$. Given the complexity of the loop decomposition, it is not clear that Eq. (4.2) would hold in this case. However, although we assume Eq. (4.2) here to make the scattering setup clearer, it is a stronger assumption than necessary; for our arguments below, it suffices to assume that $U(t)$ is amenable to a scattering treatment (with any number of consecutive sites being chosen to define a disordered sample). We have verified this assumption numerically in a simple example of the more natural disorder setup (see Appendix C).

We fix t and consider the scattering problem for $U(t)$. Incoming and outgoing waves in the leads are described by scattering amplitudes (complex numbers), and these amplitudes are related by the S matrix of the sample (a unitary matrix denoted $\mathcal{S}_{1\dots N}$). We focus on the case that the S matrix is 2×2 . Then, there are four scattering amplitudes that may be labeled as Ψ_α^\pm ($\alpha = L, R$), where $+$ ($-$) refers to right-moving (left-moving) waves and L and R refer to the left and right leads. The scattering amplitudes are related by

$$\begin{pmatrix} \Psi_R^+ \\ \Psi_L^- \end{pmatrix} = \mathcal{S}_{1\dots N} \begin{pmatrix} \Psi_L^+ \\ \Psi_R^- \end{pmatrix}. \quad (4.3)$$

Below, we argue that the 2×2 case suffices to cover a wide class of drives, and we also provide a more explicit definition of the four scattering amplitudes.

The S matrix may be parametrized by transmission and reflection amplitudes:

$$\mathcal{S}_{1\dots N} = \begin{pmatrix} t_{1\dots N} & r'_{1\dots N} \\ r_{1\dots N} & t'_{1\dots N} \end{pmatrix}. \quad (4.4)$$

In the scattering setup, localization manifests as the exponential decay of the typical transmission coefficient $T_{1\dots N} \equiv |t_{1\dots N}|^2 = |t'_{1\dots N}|^2$ as N increases: $T_{1\dots N}^{(\text{typical})} \sim e^{-2N/L_{\text{loc}}}$. From the theory of disordered systems in one

dimension, the distribution of $T_{1\dots N}$ over disorder realizations becomes log-normal for large N , and hence it is the average of the logarithm of the transmission coefficient that determines the typical value. In particular, we have

$$\frac{2}{L_{\text{loc}}} = \lim_{N \rightarrow \infty} \frac{1}{N} \langle -\ln T_{1\dots N} \rangle_{1\dots N}. \quad (4.5)$$

Unless $T_{1\dots N} = 0$ (which we assume can only occur on a set of measure zero among disorder realizations), the basic relation (4.3) can also be written in terms of the scattering transfer matrix $\mathcal{T}_{1\dots N}$ as

$$\begin{pmatrix} \Psi_R^+ \\ \Psi_L^- \end{pmatrix} = \mathcal{T}_{1\dots N} \begin{pmatrix} \Psi_L^+ \\ \Psi_R^- \end{pmatrix}. \quad (4.6)$$

The unitarity of the S matrix is equivalent to the following pseudounitarity condition:

$$\mathcal{T}_{1\dots N}^\dagger \sigma^z \mathcal{T}_{1\dots N} = \sigma^z. \quad (4.7)$$

For later use, let us recall here the general parametrization of a scattering transfer matrix:

$$\mathcal{T}_{1\dots N} = \begin{pmatrix} 1/t_{1\dots N}^* & r'_{1\dots N}/t'_{1\dots N} \\ -r_{1\dots N}/t'_{1\dots N} & 1/t'_{1\dots N} \end{pmatrix}. \quad (4.8)$$

The basic tool in our arguments below is the following formula from Refs. [42] and [43], which (as discussed there) is a corollary to the result from Schrader *et al.* [38] that we used in Sec. III A 2. The formula applies to the case of scattering that factorizes into a product of individual scattering events with i.i.d. disorder. In particular, suppose that the scattering transfer matrix of the sample can be written in the product form

$$\mathcal{T}_{1\dots N} = \mathcal{T}_{N_s} \dots \mathcal{T}_1, \quad (4.9)$$

where each \mathcal{T}_j is a 2×2 scattering transfer matrix [i.e., it satisfies Eq. (4.7)] and where N_s is the number of scattering events. (In the simplest case, $N_s = N$, but we later consider the more general case of $N_s \leq N$.) Suppose further that the entries of \mathcal{T}_j ($j = 1, \dots, N_s$) are i.i.d.; note that this amounts to assuming that the disorder in $U(t)$ is uncorrelated in space and sufficiently short-ranged. Let \mathcal{T}_j be parametrized as in Eq. (4.8) (in particular, with reflection amplitudes r_j and r'_j and reflection coefficient $R_j = |r_j|^2 = |r'_j|^2$). Then we have [44]

$$\frac{2}{L_{\text{loc}}} = \langle R_j \rangle_j - 2\text{Re} \left[\frac{\langle r_j \rangle_j \langle r'_j \rangle_j}{1 + \langle r_j r'_j / R_j \rangle_j} \right] + O(|r_j|^3), \quad (4.10)$$

where the angle brackets indicate the disorder average over any $j = 1, \dots, N_s$. (We emphasize that the index j generally stands for the disorder variables of a number of consecutive lattice sites.)

The key point is that both terms on the right-hand side are of second order in $|r_j| = |r'_j|$. Thus, provided we

can bring the scattering problem to the above form, it suffices to show $|r_j| \sim \Delta t$, for then Eq. (4.10) yields the exponent $\nu = 2$ in Eq. (2.16).

We separate the argument into two main parts. First, we consider a particular model: the SSH-type drive with on-site disorder (the same model from Sec. III, now with scattering boundary conditions). This model serves as a soluble starting point for later generalization. We obtain the required factorization into scattering transfer matrices, and we thus recover the analytical expression (3.15) for the inverse localization length that we obtained above using a position-space approach. In this simple problem, the number of scatterers is the same as the number of sites in the disordered sample: $N_s = N$.

Second, we argue that the exponent $\nu = 2$ can be obtained in a wider class of drives. Here we make the following modification (described in more detail below) to the scattering setup: We take the sample to consist of an alternating sequence of disordered regions and clean regions, with the disordered sites being a fixed fraction f of the total number of sites in the sample. Note that setting $f = 1$ would recover the scattering problem as stated above. In this setting, we obtain the exponent $\nu = 2$ for any value $0 < f < 1$ by taking the scatterers in (4.9) to be the disordered regions within the sample (hence, $N_s < N$ in this case). Equation (4.10) becomes more difficult to evaluate explicitly, so we do not obtain any formula for the nonuniversal prefactor in Eq. (2.16); however, we still obtain $|r_j| \sim \Delta t$ and hence $\nu = 2$. We also state the assumption that would be needed to obtain $\nu = 2$ in the limit $f \rightarrow 1$.

A. Scattering calculation for the SSH-type drive with on-site disorder

We consider the clean drive, as defined in Sec. III, on an infinite lattice. It is straightforward to modify the

phase disorder and bond disorder constructions of Sec. III A to the scattering setup, as we now show.

For phase disorder, we set the phases $\phi_{n,A} = \phi_{n+1,B} = 0$ except for n in the sample ($n = 1, \dots, N$). Note that the B phase is offset by one unit; this is done to simplify the transfer matrices at the sample edges, and there is no effect on the large N behavior. For bond disorder, we set $v_n = 0$ except for $n = 1, \dots, N$. Both cases can be treated at once by using the transfer matrix defined by Eqs. (3.12) and (3.13).

We fix a time t within the drive, near but not equal to $T_{\text{drive}}/2$, and we consider an eigenstate $|\Psi_\epsilon(t)\rangle$ of $U(t)$ with quasienergy $\epsilon \neq 0$ [Eq. (2.15)]. The clean spectrum becomes gapless as $\Delta t \rightarrow 0$; for sufficiently small Δt , the spectrum is doubly degenerate, with two momenta (k and $-k$) corresponding to ϵ (see Fig. 1). The eigenstates of $U_{\text{clean}}(t)$ are Bloch waves defined by [recalling Eqs. (3.4) and (3.5)]

$$\Psi_n = u(\pm k)e^{\pm ikn}, \quad (4.11)$$

where the Bloch functions $u(\pm k)$ are two-component spinors in the sublattice basis: $u(\pm k) = (u^A(\pm k), u^B(\pm k))$. There are two bands; for definiteness, we take $\epsilon > 0$, so we are considering the upper band. (Explicit expressions are given in Appendix A 2.)

A scattering eigenstate can be written as a linear combination of Bloch waves in the leads. The coefficients are the scattering amplitudes Ψ_α^\pm from Eq. (4.3). Thus,

$$\Psi_n = \begin{cases} \Psi_L^+ u(k)e^{ik(n-1)} + \Psi_L^- u(-k)e^{-ik(n-1)} & n \leq 1 \\ \Psi_R^+ u(k)e^{ik(n-1-N)} + \Psi_R^- u(-k)e^{-ik(n-1-N)} & n \geq N+1. \end{cases} \quad (4.12)$$

Our phase conventions here (i.e., the factors of $e^{\pm ik}$ and $e^{\pm ikN}$) are chosen for convenience.

To obtain the factorization (4.9), we define a matrix Λ for converting from the basis of scattering amplitudes to the basis of position states:

$$\Lambda = \begin{pmatrix} u^A(k) & u^A(-k) \\ u^B(k) & u^B(-k) \end{pmatrix}. \quad (4.13)$$

We then have

$$\Psi_1 = \Lambda \begin{pmatrix} \Psi_L^+ \\ \Psi_L^- \end{pmatrix}, \quad (4.14a)$$

$$\Psi_{N+1} = \Lambda \begin{pmatrix} \Psi_R^+ \\ \Psi_R^- \end{pmatrix}, \quad (4.14b)$$

and hence, by Eq. (3.12), we obtain the scattering transfer matrix (4.6):

$$\mathcal{T}_{1\dots N} = \Lambda^{-1} \mathcal{M}_N \dots \mathcal{M}_1 \Lambda. \quad (4.15)$$

We thus obtain the factorized form (4.9) with $N_s = N$

and

$$\mathcal{T}_n = \Lambda^{-1} \mathcal{M}_n \Lambda, \quad (4.16)$$

where we have identified the scatterer index j with the site index n (because $N_s = N$). It is readily checked that \mathcal{T}_n satisfies the pseudo-unitary condition (4.7).

To apply Eq. (4.10), we parametrize \mathcal{T}_n by r_n, r'_n , etc., as in Eq. (4.8). It is then straightforward to calculate r_n and r'_n and to then use Eq. (4.10) to again obtain the leading order expression (3.15) (see Appendix A 3 b for details).

There is a simpler way to recover Eq. (3.15): we note that \mathcal{M}_n itself satisfies the pseudo-unitarity condition (i.e., we have $\mathcal{M}_n^\dagger \sigma^z \mathcal{M}_n = \sigma^z$). We can thus consider an auxiliary problem which is defined by taking the scattering transfer matrix for the sample to be

$$\tilde{\mathcal{T}}_{1\dots N} = \tilde{\mathcal{T}}_N \dots \tilde{\mathcal{T}}_1, \quad (4.17)$$

where $\tilde{\mathcal{T}}_n = \mathcal{M}_n$. The localization length must be the same as the original problem because the scattering transfer matrices for the sample only differ by boundary terms (see, e.g., Appendix H of Ref. [43]): $\mathcal{T}_{1\dots N} = \Lambda^{-1} \tilde{\mathcal{T}}_{1\dots N} \Lambda$. We parametrize $\tilde{\mathcal{T}}_n$ by $\tilde{r}_n, \tilde{r}'_n$, etc., as in Eq. (4.8). From Eq. (3.13), we see that $\tilde{r}_n = -ie^{i(\epsilon t + \phi_{n,A})} \sin(v_n \Delta t)$ and $\tilde{r}'_n = ie^{i(\epsilon t + \phi_{n+1,B})} \sin(v_n \Delta t)$; then applying Eq. (4.10) and expanding in Δt indeed recovers Eq. (3.15).

As an aside, we consider the special case of full phase disorder, i.e., $\phi_{n,A}$ and $\phi_{n,B}$ are i.i.d. in $[-\pi, \pi)$ (and all $v_n = 1$). We can then calculate the localization length for arbitrary t via the uniform phase formula [45]: $2/L_{\text{loc}}(t) = \langle -\ln \tilde{T}_n \rangle_n$, where \tilde{T}_n is the transmission coefficient of the auxiliary problem (see Appendix A 3 c for details). The result is

$$1/L_{\text{loc}}(t) = |\ln \cos \Delta t|, \quad (4.18)$$

which agrees with numerics (Fig. 4). An equivalent formula to (4.18) has been obtained in related calculations for discrete-time quantum walks [19, 20].

B. Generalization to other drives

The calculation of the previous section has some features that are not representative of the generic case. First, the disordered unitary $U(t)$ there only couples nearest neighbors, while for a generic drive, $U(t)$ can extend further (generally it decays exponentially). Second, the clean unitary $U_{\text{clean}}(t)$ of the SSH-type drive is non-generic both in its band structure and its lack of eigenstates with complex momenta (see below).

We argue that the universal exponent $\nu = 2$ is still obtained even if both of these features are relaxed. Without claiming to establish this result rigorously, we present a sequence of generalizations beyond the soluble model of

the previous section, indicating the assumptions needed

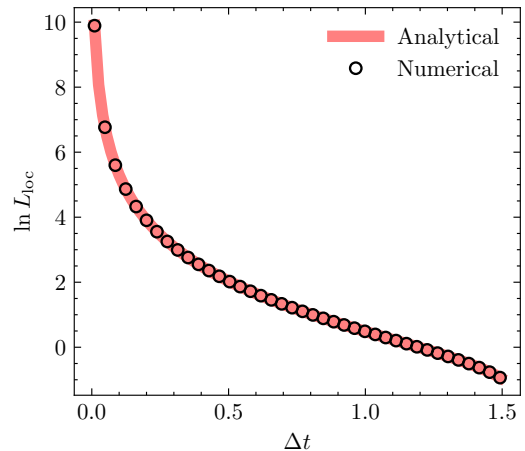


FIG. 4: The localization length $L_{\text{loc}}(t)$ at quasienergy $\epsilon = 0.57$ in the SSH-type drive with full phase disorder. The numerical results match the analytical expression (4.18). For each value of Δt , a single realization of disorder was used, and $L_{\text{loc}}(t)$ was calculated by obtaining the slope s of a linear fit for $-\ln \tilde{T}_{1\dots N}$ vs N [in the auxiliary problem defined by Eq. (4.17)], and using the relation $s = \frac{2}{L_{\text{loc}}(t)}$.

at each step. Mainly, we need to modify the original scattering problem by making the disordered sample have some arbitrarily small fraction of clean regions, and we need to make assumptions about the band structure of $U_{\text{clean}}(t)$.

a. Beyond nearest neighbors. Let us first consider the generalization to disorder that connects sites beyond nearest neighbors. Here, we continue to take $U_{\text{clean}}(t)$ to be the SSH-type drive as defined above. We assume for now that the disordered drive $U(t)$ is strictly local; that is, there some range ξ_{strict} for which

$$U_{nn'}(t) = 0 \quad (|n - n'| > \xi_{\text{strict}}), \quad (4.19)$$

where we suppress sublattice indices and any other on-site degrees of freedom. (We later make a heuristic generalization to the case of exponential locality.) Also, we assume that the constant ξ_{strict} is independent of t . The dimer disorder from Sec. III B provides an example of a drive with $\xi_{\text{strict}} = 2$.

Due to the strict locality condition (4.19), the disordered unitary agrees exactly with the clean unitary throughout the leads, except for regions of size ξ_{strict} at the edges of the sample. A scattering eigenstate can therefore be written in the leads as a linear combination of Bloch waves, provided that the edge regions are avoided. In anticipation of later generalizations, let us define $k_{\pm} = \pm k$ and $\ell_{\text{max}} = \xi_{\text{strict}}$. Then, a scattering eigenstate of $U(t)$ may be written in the leads as

$$\Psi_n = \begin{cases} \Psi_L^+ u(k_+) e^{ik_+(n-1)} + \Psi_L^- u(k_-) e^{ik_-(n-1)} & n < 1 - \ell_{\max} \\ \Psi_R^+ u(k_+) e^{ik_+(n-N)} + \Psi_R^- u(k_-) e^{ik_-(n-N)} & n > N + \ell_{\max}. \end{cases} \quad (4.20)$$

The S matrix and scattering transfer matrix of the sample are 2×2 . We would like to use the analytical result (4.10), but we face the difficulty that, due to the higher range of $U(t)$ in the disordered region, the scattering transfer matrix cannot be written in the factorized form (4.9) with i.i.d., 2×2 scattering transfer matrices \mathcal{T}_n . (Note that a factorized form with 2×2 matrices may exist, but the disorder will generally not separate. The dimer disorder model of Sec. III B illustrates this; though we worked in position space there, the scattering formulation would be similar.)

We can overcome this difficulty in a modified family of scattering problems. Before going into detail, let us state that the basic idea is to introduce clean regions, so the sample is replaced by an alternating sequence of disordered and clean regions (Fig. 5b).

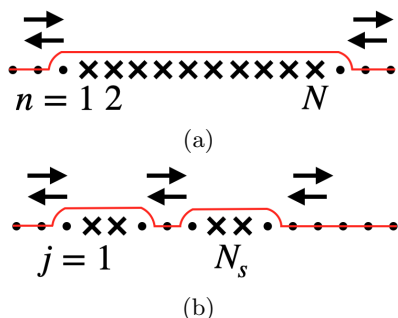


FIG. 5: Schematic of our scattering setup. Dots represent clean sites and crosses represent disordered sites. The red line indicates the magnitude of the matrix elements of the disordered unitary $U(t)$ when at least one index is a disordered site. (a) The original scattering problem, in which the disordered sites $n = 1, \dots, N$ form a disordered sample within clean leads. Here, $N = 10$. (b) A modified problem, in which we insert clean regions into the sample. There are then N_s disordered regions, each of which is a scatterer of the form of the original problem. Here, $w_{\text{block}} = 5$, $f = 2/5$, and $N_s = 2$.

Each disordered region is effectively a new sample, and in particular, has a 2×2 scattering transfer matrix. We thus obtain the factorized form (4.9). Our main task in the calculation below will be to show that we obtain the exponent $\nu = 2$ no matter how small a fraction of the overall sample is made up of clean regions. Thus, although we do not address the original problem, we do obtain the exponent in a family of problems that come arbitrarily close to the original problem.

We proceed to describe the setup in more detail. Con-

sider a sample of N lattice sites divided into blocks of size w_{block} . The total number of blocks, which we write as N_s , is then given by

$$N_s = N/w_{\text{block}}. \quad (4.21)$$

A parameter $f \in (0, 1)$ denotes the fraction of disordered sites within each block: the first $f w_{\text{block}}$ sites of each block are disordered (we refer to this group of sites as a disordered region) and the remaining $(1 - f)w_{\text{block}}$ sites are clean. Here, a site n is made clean by deleting the corresponding operator $\Theta_n(t)$ in Eq. (4.2). A unitary operator $U(f, t)$ is then defined by taking the time-ordered exponential of the Hamiltonian (4.1) from 0 to t . Setting $f = 1$ corresponds to a sample with no clean regions, which is the original scattering problem [$U(1, t) = U(t)$].

The idea is that the localization properties of $U(f, t)$ should be similar to those of $U(t)$, provided that $f \approx 1$. Let us note that for $f \in (0, 1)$, the modified unitary is generally *not* a loop [$U(f, T_{\text{drive}}) \neq 1$]; however, our arguments below do not require the loop condition to hold for general f .

We proceed to define the localization length, given any fixed fraction $f \in (0, 1)$ and any block size w_{block} . At any $t \neq T_{\text{drive}}/2$, localization occurs and has the following effect: If we increase N_s [with N determined by Eq. (4.21)], the typical transmission coefficient of the auxiliary problem decays exponentially in N_s . We may write this decay as $T_{\text{typ}} \sim e^{-2N_s w_{\text{block}}/L_{\text{loc}}(f, t)}$, where the factor of w_{block} is included so $L_{\text{loc}}(f, t)$ is measured in units of the original lattice spacing. (As usual, we are considering the localization length at some quasienergy. The localization length also depends on w_{block} , but below we will take w_{block} to be determined by f .)

We now show that at any fixed fraction $f \in (0, 1)$, the exponent $\nu = 2$ is obtained for $L_{\text{loc}}(f, t)$. Given f , we first fix a value for w_{block} that is large enough to prevent any neighboring disordered regions from overlapping. In particular, we require

$$(1 - f)w_{\text{block}} > 2\ell_{\max}. \quad (4.22)$$

We can then write the scattering wavefunction as a linear combination of Bloch waves in all of the clean regions. We follow the same phase convention as in Eq. (4.20). To do this, it is convenient to write the leftmost and rightmost site in the j th disordered region as

$$n_{L,j} = w_{\text{block}}(j - 1) + 1, \quad (4.23a)$$

$$n_{R,j} = n_{L,j} + f w_{\text{block}} - 1. \quad (4.23b)$$

Then we may write, for any $j = 1, \dots, N_s$,

$$\Psi_n = \begin{cases} \Psi_{L,j}^+ u(k_+) e^{ik_+(n-n_{L,j})} + \Psi_{L,j}^- u(k_-) e^{ik_-(n-n_{L,j})} & n_{R,j-1} + \ell_{\max} < n < n_{L,j} - \ell_{\max} \\ \Psi_{R,j}^+ u(k_+) e^{ik_+(n-n_{R,j})} + \Psi_{R,j}^- u(k_-) e^{ik_-(n-n_{R,j})} & n_{R,j} + \ell_{\max} < n < n_{L,j+1} - \ell_{\max}, \end{cases} \quad (4.24)$$

where $n_{R,0} \equiv -\infty$ and $n_{L,N_s+1} \equiv \infty$. Comparing to Eq. (4.20), we get $\Psi_L^\pm = \Psi_{L,1}^\pm$ and $\Psi_R^\pm = \Psi_{R,N_s}^\pm$. Also, comparing j to $j+1$ in Eq. (4.24), we get

$$\begin{pmatrix} \Psi_{L,j+1}^+ \\ \Psi_{L,j+1}^- \end{pmatrix} = \begin{pmatrix} e^{ik_+[(1-f)w_{\text{block}}+1]} & 0 \\ 0 & e^{ik_-[(1-f)w_{\text{block}}+1]} \end{pmatrix} \begin{pmatrix} \Psi_{R,j}^+ \\ \Psi_{R,j}^- \end{pmatrix}, \quad (4.25)$$

where we have noted that $n_{L,j+1} - n_{R,j} = (1-f)w_{\text{block}} + 1$.

The scattering transfer matrix that relates $\Psi_{L,j}^\pm$ to $\Psi_{R,j}^\pm$ is just the scattering transfer matrix of the original problem with a different number of sites ($f w_{\text{block}}$ sites instead of N). Let us write this matrix as $\hat{\mathcal{T}}_j$, bearing in mind that the subscript j stands for dependence on all of the disorder variables that appear in the j th disordered region. We then have

$$\begin{pmatrix} \Psi_{R,j}^+ \\ \Psi_{R,j}^- \end{pmatrix} = \hat{\mathcal{T}}_j \begin{pmatrix} \Psi_{L,j}^+ \\ \Psi_{L,j}^- \end{pmatrix}. \quad (4.26)$$

Collecting the last several equations, we obtain the de-

sired factorization (4.9) with

$$\mathcal{T}_j = \hat{\mathcal{T}}_j \begin{pmatrix} e^{ik_+[(1-f)w_{\text{block}}+1]} & 0 \\ 0 & e^{ik_-[(1-f)w_{\text{block}}+1]} \end{pmatrix}, \quad (4.27)$$

in which the matrix multiplying on the right only introduces unimportant phase factors. By construction, the disorder dependence in the matrices $\mathcal{T}_1, \dots, \mathcal{T}_{N_s}$ is i.i.d. because the disordered regions have no overlap. Thus, Eq. (4.10) applies. In particular, in units of the original lattice spacing, we have

$$2/L_{\text{loc}}(f, t) = \frac{1}{w_{\text{block}}} \left(\langle R_j \rangle_j - 2\text{Re} \left[\frac{\langle r_j \rangle_j \langle r'_j \rangle_j}{1 + \langle r_j r'_j / R_j \rangle_j} \right] \right) + O(|r_j|^3). \quad (4.28)$$

To complete the calculation, we next argue that the reflection amplitude of an individual block satisfies $|r_j| \sim \Delta t$. The essential point is to show $|\hat{r}_j| \sim \Delta t$, where \hat{r}_j is the reflection amplitude associated with $\hat{\mathcal{T}}_j$; once this is shown, we can easily account for the time dependence introduced by the phase factors that appear in Eq. (4.27). Indeed, from Eq. (4.27) and the general parametrization (4.8), we get

$$r_j = \hat{r}_j e^{i(k_+ - k_-)[(1-f)w_{\text{block}}+1]}, \quad (4.29a)$$

$$r'_j = \hat{r}'_j. \quad (4.29b)$$

From (4.22), we see that it suffices to take w_{block} to be, e.g., $3\ell_{\max}/(1-f)$; in particular, $(1-f)w_{\text{block}}$ is then independent of t . The momenta k_\pm depend on t in a regular way, i.e., $k_\pm = k_\pm^{(0)} + O(\Delta t)$. Thus, we conclude that $|r_j| \sim \Delta t$ will follow from $|\hat{r}_j| \sim \Delta t$.

To argue that $|\hat{r}_j| \sim \Delta t$, we begin by emphasizing the difference between two limits of the original scattering problem ($f=1$): (1) If we fix $\Delta t > 0$ and send the sample size N to infinity, then the magnitude of the sample reflection amplitude goes to unity due to localization ($|r_{1\dots N}| \rightarrow 1$). This is the regime we are interested in. However, for the purpose of treating each disordered re-

gion as a version of the original problem, it is more useful to consider the following limit. (2) If we instead fix the system size N , then we have some expansion of $r_{1\dots N}$ in powers of Δt . We claim that this expansion generically starts at first order, i.e., $r_{1\dots N} \sim \Delta t$.

The key point in our argument for (2) is our statement in Sec. II B, namely, that there are delocalized states throughout the quasienergy spectrum at $\Delta t = 0$. In the scattering framework, a state is delocalized if and only if its reflection amplitude vanishes; that is, the disorder can only appear in the transmission phases. Thus, at each quasienergy, there must be a state with $r_{1\dots N}|_{\Delta t=0} = 0$. This shows that there is no zeroth order term in the expansion of $r_{1\dots N}$ in Δt .

Generically, the first non-vanishing order should be linear (Δt), essentially because $r_{1\dots N}$ is an amplitude. Indeed, recall that in static scattering problems, the reflection amplitudes generically start at linear order in the scattering potential, in the Born approximation. In Appendix D, we use the discrete-time scattering formalism, as developed in Ref. [46], to verify that $r_{1\dots N}$ indeed generically starts at linear order in Δt .

To obtain $|\hat{r}_n| \sim \Delta t$, we apply (2) to each disordered region. The size of each disordered region ($f w_{\text{block}}$) is

determined entirely by f and ℓ_{\max} ; in particular, it is independent of t . Thus, we generically have $|\hat{r}_n| \sim \Delta t$. From Eqs. (4.10), we thus obtain $1/L_{\text{loc}}(f, t) \sim (\Delta t)^2$, i.e., $\nu = 2$ holds for any $f \in (0, 1)$.

Throughout the above argument, we have assumed $U(t)$ to be strictly local [Eq. (4.19)]. However, a generic drive is only exponentially local, i.e., for sufficiently large $|n - n'|$ we have

$$|U_{nn'}(t)| \leq C(t)e^{-|n-n'|/\xi(t)} \quad (4.30)$$

for some constants $C(t)$ and $\xi(t)$ that are independent of n, n' . We assume that we can replace $C(t) \rightarrow C$ and $\xi(t) \rightarrow \xi$ for some t -independent constants C and ξ . Then, we repeat the above arguments with ℓ_{\max} fixed to any particular value satisfying $\ell_{\max} \gg \xi$. Although the disordered unitary then differs slightly from the clean unitary even in the clean regions, the difference can be made arbitrarily small.

Finally, let us state what would need to be shown to obtain the exponent $\nu = 2$ in the original scattering problem. Our argument above yields the small Δt expansion $1/L_{\text{loc}}(f, t) = \frac{A(f)}{w_{\text{block}}}(\Delta t)^2$ for some unknown function $A(f)$. Noting from (4.22) that $w_{\text{block}} \rightarrow \infty$ as $f \rightarrow 1$, we see that $\nu = 2$ can be obtained in the limit $f \rightarrow 1$ given the assumption that $A(f) \sim w_{\text{block}}$.

b. Generalization of the clean drive. We next generalize $U_{\text{clean}}(t)$ beyond the particular case of the SSH-type drive. Here we note that the precise forms of the Bloch function $u(k)$ and of the two momenta k_{\pm} were not important in our calculation above; the essential point was that the S matrix for the sample was 2×2 . We can therefore generalize our calculation to include any quasienergy at which $U_{\text{clean}}(t)$ has two-fold degeneracy for all t in some neighborhood of $T_{\text{drive}}/2$.

Let us consider the case that $U_{\text{clean}}(t)$ has two bands, which we write as $\epsilon_{\pm}(t, k)$. In momentum space, the block-diagonal form (2.12) becomes

$$U_{\text{clean}}(T_{\text{drive}}/2, k) = \begin{pmatrix} U_{AA}(k) & 0 \\ 0 & U_{BB}(k) \end{pmatrix}, \quad (4.31)$$

where, by assumption, $U_{AA}(k)$ and $U_{BB}(k)$ have winding numbers 1 and -1 , respectively. The corresponding quasienergy spectra $\epsilon_A(k)$ and $\epsilon_B(k)$ must go from $\epsilon = -2\pi/T_{\text{drive}}$ to $2\pi/T_{\text{drive}}$, but need not do so monotonically. Example spectra are sketched in Fig. 6.

For t close to but not equal to $T_{\text{drive}}/2$, gaps open at all band crossings. We define $\epsilon_+(k)$ and $\epsilon_-(k)$ to be the upper and lower bands, respectively, and we focus for now on the midpoint of the drive, at which the bands $\epsilon_{\pm}(k)$ are defined by taking the limit as $t \rightarrow T_{\text{drive}}/2$. [Note that the bands $\epsilon_{\pm}(k)$ at the midpoint are not the same as $\epsilon_A(k)$ and $\epsilon_B(k)$.] As is clear from Fig. 6, there is generically some *range* of quasienergies ϵ that have a two-fold degeneracy with the two associated momenta moving in opposite directions. It is for ϵ in this range that our argument straightforwardly applies.

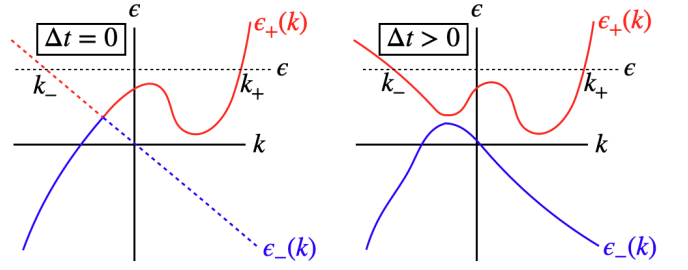


FIG. 6: Illustration of the band structure of a more general two-band drive $U_{\text{clean}}(t)$. A particular quasienergy ϵ is fixed, while Δt is varied. Left: The midpoint of the drive ($\Delta t = 0$). The solid line is $\epsilon_A(k)$ and the dashed line is $\epsilon_B(k)$; they reflect the winding numbers (1 and -1) of $U_{AA}(k)$ and $U_{BB}(k)$. Though some quasienergies have higher degeneracy, there is a range of quasienergies that have two-fold degeneracy, with one right mover (k_+) and one left mover (k_-). Right: Small, non-zero Δt . The values of k_+ and k_- depend on Δt , but there remains a similar range of quasienergies with twofold degeneracy.

Let us explain this in more detail. For ϵ in some range, we have $\epsilon = \epsilon_+(k_-) = \epsilon_+(k_+)$, $v_g(k_+) > 0$, and $v_g(k_-) < 0$, where $v_g(k) = \partial\epsilon_+(k)/\partial k$ is the group velocity. (Here we assume for definiteness that ϵ lies in the upper band.) Although we have considered $\epsilon_{\pm}(k)$ at the midpoint ($t = T_{\text{drive}}/2$), allowing t to vary slightly from the midpoint does not change the qualitative features; there remains a similar range of quasienergies with the desired two-fold degeneracy. For quasienergies in this range, and for t sufficiently close to the midpoint, the eigenstates of $U_{\text{clean}}(t)$ are linear combinations of two (time-dependent) Bloch waves. We have thus brought our localization problem, for a more general class of topologically nontrivial drives, into the framework of scattering with 2×2 matrices, at least for some range of quasienergies.

We now present the scattering argument for the exponent $\nu = 2$ in this more general setting. A complication arises, both in the basic setup of the scattering problem and in our argument about inserting clean regions: although by assumption $U_{\text{clean}}(t)$ has two bands, it may have eigenstates with complex momenta when confined either to a half-line or to a finite region. These eigenstates grow or decay exponentially in position space; schematically, $\langle n | \Psi_{\epsilon}(t) \rangle \sim e^{\pm n/r_{\epsilon}(t)}$ for some decay length $r_{\epsilon}(t)$. [We emphasize that this length scale is distinct from the operator decay length $\xi(t)$ that appears in Eq. (4.30). Even a strictly local $U_{\text{clean}}(t)$ can have exponentially decaying eigenstates, although the SSH-type drive of Sec. III does not.] When we introduce disorder into sites $n = 1, \dots, N$, the edge sites ($n = 1$ and N) can then be regarded as endpoints of half-lines that extend into the leads. This implies that the eigenstate wavefunction in the leads is generally not a linear combination solely of Bloch waves [even at distances greater than $\xi(t)$ away

from the sample]; there can also be contributions from modes that decay as $n \rightarrow \pm\infty$. The solution is simple: as usual in scattering theory, the expansion in terms of Bloch waves [Eq. (4.20)] holds for $n \rightarrow \pm\infty$.

Similarly, we must note that the exponentially growing and decaying eigenstates of $U_{\text{clean}}(t)$ can appear in each inserted clean region [even at distances greater than $\xi(t)$ from the nearest disordered region]. To deal with this, we assume that the decay lengths of the eigenstates of $U_{\text{clean}}(t)$ can be uniformly bounded, in the sense that there is a fixed distance r_ϵ , independent of t , for which $r_\epsilon(t) < r_\epsilon$ for all t (in some neighborhood of $T_{\text{drive}}/2$). We choose the constant ℓ_{max} to be much greater than r_ϵ , i.e., ℓ_{max} satisfies

$$\ell_{\text{max}} \gg \max\{\xi, r_\epsilon\}. \quad (4.32)$$

Then, the expansions in terms of Bloch waves—both the basic setup [Eq. (4.20)] and the more general expansions within each clean region [Eq. (4.24)]—hold as written (up to error that can be decreased arbitrarily by increasing ℓ_{max}). From this point onward, our argument for the exponent $\nu = 2$ proceeds exactly as in the case that $U_{\text{clean}}(t)$ was taken to be the SSH-type drive.

Thus, we have obtained the exponent $\nu = 2$ provided that we consider a quasienergy ϵ at which the clean drive (evaluated at the midpoint) has twofold degeneracy. In the generic two-band case, there is a range of ϵ for which this condition holds.

V. CONCLUSION

We considered the class AIII of Floquet drives in one spatial dimension, focusing on drives with topological index equal to one. We argued that these drives exhibit a localization-delocalization transition, with the localization length diverging throughout the quasienergy spectrum at a particular time (the midpoint of the loop part of the drive). We obtained the delocalization exponent $\nu = 2$ explicitly in a simple model, checked it numerically in more complicated models, and provided an analytical argument for a class of models (based on some plausible assumptions). We expect that some assumptions of the analytical argument are not essential; for instance, the restriction to twofold degeneracy in the clean drive. Also, we expect that the same exponent holds for any nonzero value of the topological index.

A basic assumption throughout this work is the chiral symmetry, which relates the Hamiltonian to itself at different times. Since we focus on disordered systems, this symmetry property could be difficult to achieve in a real system. To address this, it would be interesting to see if the exponent persists even if the symmetry holds only in a disorder-averaged sense rather than holding for every disorder realization [47]. Alternatively, the setup we discuss at the end of Sec. IID, which yields the same exponent without appeal to a time-dependent symmetry constraint, could be explored further.

Another natural follow-up to this work would be to consider the effect of interactions. The SSH-type drive we have considered readily extends to an interacting spin model; note also that the interacting generalization of the flow index is known from Ref. [34]. The interacting generalization of our work may provide an interesting example of a localization-delocalization transition in a Floquet-many-body-localized setting.

ACKNOWLEDGMENTS

We thank Victor Gurarie, Curt von Keyserlingk, and Shivaji Sondhi for useful discussions on related topics. This work used computational and storage services associated with the Hoffman2 Shared Cluster provided by UCLA Institute for Digital Research and Education's Research Technology Group. A.B.C., P.S., and R.R. acknowledge financial support from the University of California Laboratory Fees Research Program funded by the UC Office of the President (UCOP), grant number LFR-20-653926. A.B.C. acknowledges financial support from the Joseph P. Rudnick Prize Postdoctoral Fellowship (UCLA). P.S. acknowledges financial support from the Center for Quantum Science and Engineering Fellowship (UCLA) and the Bhaumik Graduate Fellowship (UCLA). P.S. acknowledges the support of NNSA for the U.S. DoE at LANL under Contract No. DE-AC52-06NA25396, and Laboratory Directed Research and Development (LDRD) for support through 20240032DR. LANL is managed by Triad National Security, LLC, for the National Nuclear Security Administration of the U.S. DOE under contract 89233218CNA000001. Research presented in this article was also supported by the National Security Education Center (NSEC) Informational Science and Technology Institute (ISTI) using the Laboratory Directed Research and Development program of Los Alamos National Laboratory project number 20240479CR-IST.

Appendix A: Further details for the SSH-type drive with on-site disorder

1. Mapping to discrete-time quantum walk

In the main text, we showed that the eigenstate problem [Eq. (2.15)] becomes Eqs. (3.11a) and (3.11b) in position space. Here, we show that these equations are equivalent to a special case of the generalized discrete-time quantum

walk studied in Ref. [19]. We start by reviewing the setup for the discrete-time quantum walk [19].

The discrete-time quantum walk occurs on an infinite chain with a two-component ‘‘spin’’ degree of freedom (\uparrow, \downarrow) at each site; a general state is written as $|\Psi\rangle = \sum_n (\Psi_{n,\uparrow} |n, \uparrow\rangle + \Psi_{n,\downarrow} |n, \downarrow\rangle)$. A single time step is implemented by a unitary operator $\hat{U} = \hat{S}\hat{U}_{\text{coin}}$, where the shift \hat{S} moves up (down) spins one unit to the right (left) and where \hat{U}_{coin} acts on the spin degree of freedom at each site n as a unitary 2×2 matrix $U_{\text{coin},n}$. The matrix $U_{\text{coin},n}$ is parameterized by $\varphi_n, \varphi_{1,n}, \varphi_{2,n}$, and θ_n (in the same way as in Eq. (1) of Ref. [19]).

The eigenstate equation for the discrete-time quantum walk problem is $\hat{U}|\Psi\rangle = e^{-i\omega}|\Psi\rangle$. In position space, the eigenstate equations become Eqs. (H1a) and (H2b) of Ref. [43]. Our Eqs. (3.11a) and (3.11b) are in fact special cases of (H1a) and (H2b) [with n relabelled as $n-1$ in (H1a) and as $n+1$ in (H2b)] with the following choice of parameters:

$$\varphi_n = \frac{1}{2}(\phi_{n,A} + \phi_{n+1,B}), \quad (\text{A1a})$$

$$\varphi_{1,n} = \frac{1}{2}(\phi_{n,A} - \phi_{n+1,B}), \quad (\text{A1b})$$

$$\varphi_{2,n} = -\frac{1}{2}(\phi_{n,A} - \phi_{n+1,B}) + \pi/2, \quad (\text{A1c})$$

$$\theta_n = v_n \Delta t, \quad (\text{A1d})$$

and with the following correspondence of the basic variables:

$$\Psi_{n,\uparrow} \leftrightarrow \Psi_{n,A}, \quad \Psi_{n-1,\downarrow} \leftrightarrow \Psi_{n,B}, \quad \omega \leftrightarrow \epsilon t. \quad (\text{A2})$$

Using this mapping, we can reproduce some of the results below by translating results from the discrete-time quantum walk case. However, for completeness we present the calculations directly in the case of the SSH-type drive.

2. Solution of the clean model

By Bloch’s theorem, a wavefunction that solves the eigenstate equation (2.15) with some quasienergy $\epsilon(k)$ can be written as

$$\Psi_n = u(k)e^{ikn}, \quad (\text{A3})$$

where the Bloch function $u(k)$ is a two-component spinor in the sublattice index:

$$u(k) \equiv \begin{pmatrix} u_A(k) \\ u_B(k) \end{pmatrix}. \quad (\text{A4})$$

We proceed to solve for the quasienergies and Bloch functions. From now on, we assume that are in the middle section of the drive ($T_{\text{drive}}/ < t < 3\pi/2$). We remove the disorder from Eqs. (3.8a) and (3.8b) (by setting all $\phi_{n,A} = \phi_{n,B} = 0$) to obtain

$$\cos(\Delta t) \Psi_{n-1,A} + i \sin(\Delta t) \Psi_{n,B} = e^{-i\epsilon t} \Psi_{n,A}, \quad (\text{A5a})$$

$$i \sin(\Delta t) \Psi_{n,A} + \cos(\Delta t) \Psi_{n+1,B} = e^{-i\epsilon t} \Psi_{n,B}. \quad (\text{A5b})$$

Substituting in the plane wave form given above, we obtain

$$\begin{pmatrix} e^{-ik} \cos(\Delta t) & i \sin(\Delta t) \\ i \sin(\Delta t) & e^{ik} \cos(\Delta t) \end{pmatrix} u(k) = e^{-i\epsilon(k)t} u(k), \quad (\text{A6})$$

which we then solve to find the two bands of the model (denoted $+$ and $-$). The quasienergies of the two bands are defined (modulo $2\pi/t$) by

$$e^{-i\epsilon_{\pm}(k)t} = \cos(\Delta t) \cos k \mp i \sqrt{1 - \cos^2 \Delta t \cos^2 k}, \quad (\text{A7})$$

and the unit-normalized Bloch spinors are

$$u_{\pm}(k) = \frac{\text{sgn } k}{\mathcal{N}_{\pm}(k)} \begin{pmatrix} \sin(\Delta t) \\ \cos(\Delta t) \sin k \mp \sqrt{1 - \cos^2 \Delta t \cos^2 k} \end{pmatrix}, \quad (\text{A8})$$

where the prefactor of $\text{sgn } k$ is chosen for convenience and where $\mathcal{N}_\pm(k)$ is a normalization factor:

$$\mathcal{N}_\pm(k) = \sqrt{2 \left(1 - \cos^2 \Delta t \cos^2 k \mp \cos(\Delta t) \sin k \sqrt{1 - \cos^2 \Delta t \cos^2 k} \right)}. \quad (\text{A9})$$

The first Brillouin zone is $|k| < \pi$ and $\epsilon_\pm(k)$ is fixed by requiring $|\epsilon_\pm(k)t| < \pi$. The resulting two bands are shown in Fig 1.

3. Calculation of the localization length

a. Position space calculation

Here we obtain Eq. (3.15) using a result from Schrader *et al.* [38]. For a summary of their setup in a notation similar to that used in this paper, and also for a calculation that includes that below as a special case (using the mapping from Appendix A 1), see Appendix B of Ref. [43].

As we point out in the main text, the (position-space) transfer matrix \mathcal{M}_n satisfies $\mathcal{M}_n^\dagger \sigma^z \mathcal{M}_n = \sigma^z$. Reference [38] instead considers matrices satisfying the same condition with σ^z replaced by σ^y ; however, as they point out, the two types of matrix are isomorphic. We therefore start by defining a matrix K_n that is isomorphic to \mathcal{M}_n : in particular, $K_n = C \mathcal{M}_n C^{-1}$, where the unitary matrix C is given by [38]

$$C \equiv \frac{1}{\sqrt{2}} \begin{pmatrix} i & i \\ 1 & -1 \end{pmatrix}. \quad (\text{A10})$$

Then K_n satisfies the σ^y condition.

Equation (3.14) can be written in terms of the K_n matrices as

$$\gamma(t) = \lim_{N \rightarrow \infty} \frac{1}{N} \langle \ln \|K_N \dots K_1\| \rangle_{1 \dots N}, \quad (\text{A11})$$

Note that in passing from Eq. (3.14) to Eq. (A11), we dropped boundary terms that make no contribution in the limit $N \rightarrow \infty$.

Reference [38] calculates (A11) to leading order in a small parameter λ which is given in our case by $\lambda = \Delta t$. To use the result from Ref. [38], we must verify that K_n (there denoted $T_{\lambda, \sigma}$) satisfies the necessary properties. First, we check that the matrices K_n commute with each other at $\Delta t = 0$. At the point $\Delta t = 0$, we have

$$\mathcal{M}_n = \begin{pmatrix} e^{i(\pi\epsilon + \phi_{n,A})} & 0 \\ 0 & e^{-i(\pi\epsilon + \phi_{n+1,B})} \end{pmatrix}, \quad (\text{A12})$$

which implies in particular that $[\mathcal{M}_n, \mathcal{M}_{n'}]_{\Delta t=0} = 0$; then the same is true for the K_n matrices, by linearity. Second, we must check the trace condition $|\text{Tr} K_n|_{\Delta t=0} < 2$, which in our case reduces to

$$|e^{i(\pi\epsilon + \phi_{n,A})} + e^{-i(\pi\epsilon + \phi_{n+1,B})}| < 2. \quad (\text{A13})$$

At worst, the left-hand side can equal 2, but only in a fine-tuned case; generically, the inequality is satisfied.

We then define

$$\eta_n = \pi\epsilon + \frac{1}{2}(\phi_{n,A} + \phi_{n+1,B}), \quad (\text{A14a})$$

$$\xi_n = \frac{1}{2}(\phi_{n,A} - \phi_{n+1,B}), \quad (\text{A14b})$$

$$P_n = \begin{pmatrix} v_n \sin(\phi_{n,A} + \pi\epsilon) & v_n \cos(\phi_{n,A} + \pi\epsilon) - \epsilon \\ v_n \cos(\phi_{n,A} + \pi\epsilon) + \epsilon & -v_n \sin(\phi_{n,A} + \pi\epsilon) \end{pmatrix}. \quad (\text{A14c})$$

Note that P_n is real and traceless. We then have, by a straightforward calculation, a parametrization of the form of Eq. (8) from Ref. [38]:

$$K_n = e^{i\xi_n} R_{\eta_n} (\mathbb{I} + \Delta t P_n) + O((\Delta t)^2), \quad (\text{A15})$$

where R_{η_n} is the 2×2 matrix that rotates by the angle η_n . [Eq. (8) in Ref. [38] also includes a matrix $M \in \text{SL}(2, \mathbb{R})$, which is in our case the identity matrix, and another matrix Q_n that is not needed for our purposes.] The constant β_n defined (in a slightly different notation) by Eq. (9) from Ref. [38] is then found to be

$$\beta_n = -iv_n e^{i(\pi\epsilon + \phi_{n,A})}. \quad (\text{A16})$$

Finally, substituting Eqs. (A14a) and (A16) into Eq. (22) of Ref. [38] yields Eq. (3.15) from the main text.

b. Scattering calculation

In Sec. IV A, we obtained the inverse localization length at leading order in Δt [Eq. (3.15)] by applying the scattering formula (4.10) to the auxiliary problem defined by Eq. (4.17). This required us to show that the auxiliary problem has the same localization length as the original problem. In this section, we apply Eq. (4.10) directly to the original problem, yielding the same result (3.15).

Without loss of generality, we fix $\epsilon > 0$ and consider $\Delta t > 0$. The scattering momentum $k > 0$ and the Bloch function $u(k)$ vary with t . Expanding in Δt , we readily obtain

$$k = \pi\epsilon + O((\Delta t)^2), \quad (\text{A17a})$$

$$u(k) = \begin{pmatrix} 1 \\ -\frac{1}{2}(\csc k)\Delta t \end{pmatrix} + O((\Delta t)^2) \quad (\text{A17b})$$

$$u(-k) = \begin{pmatrix} -\frac{1}{2}(\csc k)\Delta t \\ 1 \end{pmatrix} + O((\Delta t)^2). \quad (\text{A17c})$$

Then, from Eqs. (3.13), (4.13), and (4.16), we calculate the scattering transfer matrix \mathcal{T}_n as an expansion in Δt . We only need the reflection amplitudes at linear order in Δt , and they can be obtained straightforwardly using the general parametrization (4.8):

$$r_n = \frac{1}{2} \left(\csc k - e^{i(2k+\phi_{n,A}+\phi_{n+1,B})} \csc k + 2iv_n e^{i(k+\phi_{n,A})} \right) \Delta t + O((\Delta t)^2), \quad (\text{A18a})$$

$$r'_n = \frac{1}{2} \left(\csc k - e^{i(2k+\phi_{n,A}+\phi_{n+1,B})} \csc k + 2iv_n e^{i(k+\phi_{n+1,B})} \right) \Delta t + O((\Delta t)^2). \quad (\text{A18b})$$

Substitution into Eq. (4.10) yields Eq. (3.15) from the main text once again.

c. Full phase disorder

To obtain Eq. (4.18), we start by recalling a result from Ref. [45]. Consider a general scattering problem in which we have the factorization (4.9) with $N_s = N$ (hence we will write $\mathcal{T}_j \equiv \mathcal{T}_n$). Let \mathcal{T}_n be parametrized by r_n , r'_n , t_n , and t'_n , as in Eq. (4.8). If, at sufficiently large system size N , we have the following phase uniformity condition:

$$\text{Arg}[r'_{1\dots N} r_{N+1}] \text{ is distributed uniformly in } [-\pi, \pi], \text{ independently of } |r_{N+1}|, \quad (\text{A19})$$

then Ref. [45] shows

$$\frac{2}{L_{\text{loc}}} = \langle -\ln T_n \rangle_n, \quad (\text{A20})$$

where $T_n = |t_n|^2 = |t'_n|^2$ is the transmission coefficient and where the disorder average is taken over any site $n = 1, \dots, N$. Since $\text{Arg}[r'_{1\dots N} r_{N+1}] = \text{Arg}[r'_{1\dots N}] + \text{Arg}[r_{N+1}]$, one simple case in which the condition (A19) holds is the following: $\text{Arg}[r_n]$ is distributed uniformly in $[-\pi, \pi]$, independently of $|r_n|$.

We now apply this result to the SSH-type drive with on-site phase disorder. (We do not consider bond disorder because this was only defined for times t near the midpoint, whereas here our concern is to find an answer for all t .) It is simplest to work with the auxiliary problem defined by Eq. (4.17). Setting $v_n = 1$ in Eq. (3.13), we get $\text{Arg}[\tilde{r}_n] = \epsilon t + \phi_{n,A} + \frac{\pi}{2} \text{sgn} \Delta t$ and $|\tilde{r}_n| = |\sin \Delta t|$. Thus, if $\phi_{n,A}$ is uniformly distributed in $[-\pi, \pi]$, then the condition (A19) holds, and (A20) yields Eq. (4.18) from the main text.

Appendix B: Transfer matrix for the SSH-type drive with dimer disorder

Here we derive the transfer matrix relation (3.19a) and the explicit expression for the transfer matrix $\mathcal{M}_{n,A}$ for the A sites. To simplify the notation, we relabel the four sites $|2n-1, A\rangle$, $|2n-1, B\rangle$, $|2n, A\rangle$ and $|2n, B\rangle$ as $|n, a\rangle$, $|n, b\rangle$, $|n, c\rangle$ and $|n, d\rangle$, respectively. We write the disordered unitary matrices $U_{n,\alpha}$ ($\alpha = A$ or B) as

$$U_{n,A} = \begin{pmatrix} U_n^{aa} & U_n^{ac} \\ U_n^{ca} & U_n^{cc} \end{pmatrix}, \quad U_{n,B} = \begin{pmatrix} U_n^{bb} & U_n^{bd} \\ U_n^{db} & U_n^{dd} \end{pmatrix}. \quad (\text{B1})$$

It is straightforward to show that the eigenstate equation (2.15) becomes the following four equations in position space:

$$e^{-i\epsilon t}\Psi_{n,a} = \cos(\Delta t)(U_{n-1}^{ca}\Psi_{n-1,a} + U_{n-1}^{cc}\Psi_{n-1,c}) + i\sin(\Delta t)(U_n^{bb}\Psi_{n,b} + U_n^{bd}\Psi_{n,d}), \quad (\text{B2a})$$

$$e^{-i\epsilon t}\Psi_{n,b} = i\sin(\Delta t)(U_n^{aa}\Psi_{n,a} + U_n^{ac}\Psi_{n,c}) + \cos(\Delta t)(U_n^{db}\Psi_{n,b} + U_n^{dd}\Psi_{n,d}), \quad (\text{B2b})$$

$$e^{-i\epsilon t}\Psi_{n,c} = \cos(\Delta t)(U_n^{aa}\Psi_{n,a} + U_n^{ac}\Psi_{n,c}) + i\sin(\Delta t)(U_n^{db}\Psi_{n,b} + U_n^{dd}\Psi_{n,d}), \quad (\text{B2c})$$

$$e^{-i\epsilon t}\Psi_{n,d} = i\sin(\Delta t)(U_n^{ca}\Psi_{n,a} + U_n^{cc}\Psi_{n,c}) + \cos(\Delta t)(U_{n+1}^{bb}\Psi_{n+1,b} + U_{n+1}^{bd}\Psi_{n+1,d}). \quad (\text{B2d})$$

We use the second and third equations to eliminate $\Psi_{n,b}$ and $\Psi_{n,c}$ [this is expressed by Eq. (3.19b)]. From the first and fourth equations, we then obtain

$$\begin{pmatrix} \Psi_{n+1,a} \\ \Psi_{n+1,d} \end{pmatrix} = \mathcal{M}_{n,\text{dimer}} \begin{pmatrix} \Psi_{n,a} \\ \Psi_{n,d} \end{pmatrix}, \quad (\text{B3})$$

where the transfer matrix $\mathcal{M}_{n,\text{dimer}}$ is given below. Note that this is the same as Eq. (3.19a) from the main text.

To present the transfer matrix, we first define

$$D_n = 1 + U_n^{ac}U_n^{db}e^{2i\epsilon t} - \cos(\Delta t)(U_n^{ac} + U_n^{db})e^{i\epsilon t}, \quad (\text{B4a})$$

$$E_n = [U_n^{aa}U_n^{cc} - U_n^{ca}(U_n^{ac} + U_n^{db})]e^{i\epsilon t}, \quad (\text{B4b})$$

$$F_n = U_n^{ca} + U_n^{db}(U_n^{ac}U_n^{ca} - U_n^{aa}U_n^{cc})e^{2i\epsilon t}, \quad (\text{B4c})$$

$$G_n = U_n^{bd} + U_n^{ac}(U_n^{bd}U_n^{db} - U_n^{bb}U_n^{dd})e^{2i\epsilon t} + \cos(\Delta t)[U_n^{bb}U_n^{dd} - U_n^{bd}(U_n^{ac} + U_n^{db})]e^{i\epsilon t}. \quad (\text{B4d})$$

Then the transfer matrix is

$$\mathcal{M}_{n,\text{dimer}} = \begin{pmatrix} \mathcal{M}_{n,\text{dimer}}^{aa} & \mathcal{M}_{n,\text{dimer}}^{ad} \\ \mathcal{M}_{n,\text{dimer}}^{da} & \mathcal{M}_{n,\text{dimer}}^{dd} \end{pmatrix}, \quad (\text{B5})$$

with the following matrix elements:

$$\mathcal{M}_{n,\text{dimer}}^{aa} = \frac{[E_n + \sec(\Delta t)F_n]}{D_n}e^{i\epsilon t}, \quad (\text{B6a})$$

$$\mathcal{M}_{n,\text{dimer}}^{ad} = i\{\tan(\Delta t)[1 + (U_n^{ac}U_n^{db} + U_n^{cc}U_n^{dd})e^{2i\epsilon t}] - \sin(\Delta t)(U_n^{ac} + U_n^{db})e^{i\epsilon t}\}/D_n, \quad (\text{B6b})$$

$$\begin{aligned} \mathcal{M}_{n,\text{dimer}}^{da} &= -i\frac{\sin(\Delta t)E_n + \tan(\Delta t)F_n}{D_n G_{n+1}} \\ &\quad \times [1 + (U_{n+1}^{aa}U_{n+1}^{bb} + U_{n+1}^{ac}U_{n+1}^{db})e^{2i\epsilon t} - \cos(\Delta t)(U_{n+1}^{ac} + U_{n+1}^{db})e^{i\epsilon t}], \end{aligned} \quad (\text{B6c})$$

$$\begin{aligned} \mathcal{M}_{n,\text{dimer}}^{dd} &= \left\{ \sec(\Delta t) (1 + e^{2i\epsilon t}U_n^{ac}U_n^{db}) (1 + e^{2i\epsilon t}U_{n+1}^{ac}U_{n+1}^{db}) \right. \\ &\quad \times \cos(\Delta t)e^{i\epsilon t} \left[(U_n^{ac} + U_n^{db})(U_{n+1}^{ac} + U_{n+1}^{db}) + \sin^2(\Delta t)e^{2i\epsilon t}U_{n+1}^{aa}U_{n+1}^{bb}U_n^{cc}U_n^{dd} \right] \\ &\quad - e^{2i\epsilon t}U_{n+1}^{ac}U_n^{db}U_{n+1}^{db} - U_{n+1}^{ac} - U_{n+1}^{db} - U_n^{db} \\ &\quad - U_n^{ac} \{1 + e^{2i\epsilon t} [U_{n+1}^{ac}U_{n+1}^{db} + U_n^{db}(U_{n+1}^{ac} + U_{n+1}^{db})]\} \\ &\quad \left. - \sin^2(\Delta t)e^{2i\epsilon t} [U_{n+1}^{aa}U_{n+1}^{bb}(U_n^{ac} + U_n^{db}) + U_n^{cc}U_n^{dd}(U_{n+1}^{ac} + U_{n+1}^{db})] \right. \\ &\quad \left. + \sin(\Delta t)\tan(\Delta t)e^{i\epsilon t} \left[U_{n+1}^{aa}U_{n+1}^{bb}(1 + e^{2i\epsilon t}U_n^{ac}U_n^{db}) + U_n^{cc}U_n^{dd}(1 + e^{2i\epsilon t}U_{n+1}^{ac}U_{n+1}^{db}) \right] \right. \\ &\quad \left. + \sin^3(\Delta t)\tan(\Delta t) + e^{3i\epsilon t}U_{n+1}^{aa}U_{n+1}^{bb}U_n^{cc}U_n^{dd} \right\} / (D_n G_{n+1}). \end{aligned} \quad (\text{B6d})$$

Appendix C: Disorder remains short-ranged under loop decomposition

An important part of our scattering argument in Sec. IV is the assumption that the disorder in the loop drive is short-ranged. In this Appendix, we do some basic numerical checks to verify that this is a reasonable assumption, taking as a starting point that the disorder in the original (nonloop) drive is short-ranged.

Roughly speaking, the scenario we wish to rule out is the following. If the original drive is a finite-sized disordered sample (see below), one could question if the loop drive is also described by a finite-sized disordered sample. If instead it turns out that the loop decomposition spreads the disorder through the entire system, this would seem to make a scattering treatment impossible.

More precisely, instead of taking the loop drive to have the form of Eqs. (4.1) and (4.2), we assume that the original drive takes that form, i.e.,

$$\mathcal{H}(t) = \mathcal{H}_{\text{clean}}(t) + \mathcal{H}_{\text{disorder}}(t), \quad (\text{C1})$$

where

$$\mathcal{H}_{\text{disorder}}(t) = \sum_n \Theta'_n(t), \quad (\text{C2})$$

and each operator $\Theta'_n(t)$ is exponentially localized near the site n . We then do the loop decomposition, as described in Sec. II A, on both $\mathcal{H}(t)$ and $\mathcal{H}_{\text{clean}}(t)$; this yields loop drives $U(t)$ and $U_{\text{clean}}(t)$. To match the main text setup exactly, we would need to find that the loop Hamiltonian takes the form (4.1) and (4.2). However, this requirement may be too stringent.

A weaker condition that should still suffice for our purposes is that $U(t)$ should be suitable for a scattering treatment. In particular, if we define a disordered sample in the usual way, by setting $\Theta'_n(t) = 0$ for all $n \leq 0$ and $n \geq N + 1$, we would then like to find that $U_{nn'}(t) \rightarrow U_{\text{clean},nn'}(t)$ far from the disordered region.

We have verified this condition numerically in a particular example of a nonloop drive. We consider the SSH-type drive from the main text, generalized to have arbitrary coefficients in front of the trivial and topological SSH Hamiltonians. Thus, we define

$$\mathcal{H}_{1,\text{clean}} = h_1 \sum_n (|n, A\rangle \langle n, B| + \text{H.c.}), \quad (\text{C3a})$$

$$\mathcal{H}_2 = \mathcal{H}_{2,\text{clean}} + \mathcal{H}_{2,d}, \quad (\text{C3b})$$

$$\mathcal{H}_{2,\text{clean}} = -h_2 \sum_n (|n + 1, A\rangle \langle n, B| + \text{H.c.}), \quad (\text{C3c})$$

$$\mathcal{H}(t) = \begin{cases} \mathcal{H}_{1,\text{clean}} & 0 \leq t < \frac{T_{\text{drive}}}{4} \\ \mathcal{H}_2 & \frac{T_{\text{drive}}}{4} \leq t \leq \frac{3T_{\text{drive}}}{4} \\ \mathcal{H}_{1,\text{clean}} & \frac{3T_{\text{drive}}}{4} < t \leq T_{\text{drive}}, \end{cases} \quad (\text{C3d})$$

with $\mathcal{H}_{\text{clean}}(t)$ defined similarly (by setting $\mathcal{H}_{2,d} = 0$). For $h_1 = h_2 = 2\pi/T_{\text{drive}}$, $\mathcal{H}_{\text{clean}}(t)$ is the same as the SSH-type drive from the main text; more generally, the drive has chiral symmetry but is not a loop. We have assumed for definiteness that the disorder is only in \mathcal{H}_2 . We further specialize to the disorder being a single defect at the bond connecting two adjacent sites n_0 and $n_0 + 1$:

$$\mathcal{H}_{2,d} = h_d (|n_0 + 1, A\rangle \langle n_0, B| + \text{H.c.}). \quad (\text{C4})$$

Putting the system on a ring of L sites, we do exact diagonalization to calculate the loop drive $U(t)$ near the midpoint using Eq. (2.8) and $H_F = (i/T_{\text{drive}}) \ln \mathcal{U}(T_{\text{drive}})$. To test if the defect spreads under the loop decomposition, we examine matrix elements of the operator

$$\Delta U(t) \equiv U(t) - U_{\text{clean}}(t). \quad (\text{C5})$$

We first consider the quantity

$$\max\{|\Delta U_{n'\alpha',n\alpha}(t)|\}_{1 \leq n' \leq L} \quad (\alpha, \alpha' \in \{A, B\}) \quad (\text{C6})$$

as a function of n , finding that it is peaked at the defect (i.e., at $n = n_0$ or $n_0 + 1$). We then fix n at the peak value and confirm that $|\Delta U_{n'\alpha',n\alpha}(t)|$ decays rapidly with increasing $|n' - n|$ (Fig. 7).

We obtained similar results in the case of a phase defect, where we define a chiral-symmetric nonloop drive in the same way as in Eq. (2.21). The disordered unitary U_d is defined by setting all phases in Eq. (3.6) to zero except a single $\phi_{n_0,A}$. In this case, we again found that the loop drive differs from the clean loop drive only near the defect site n_0 .

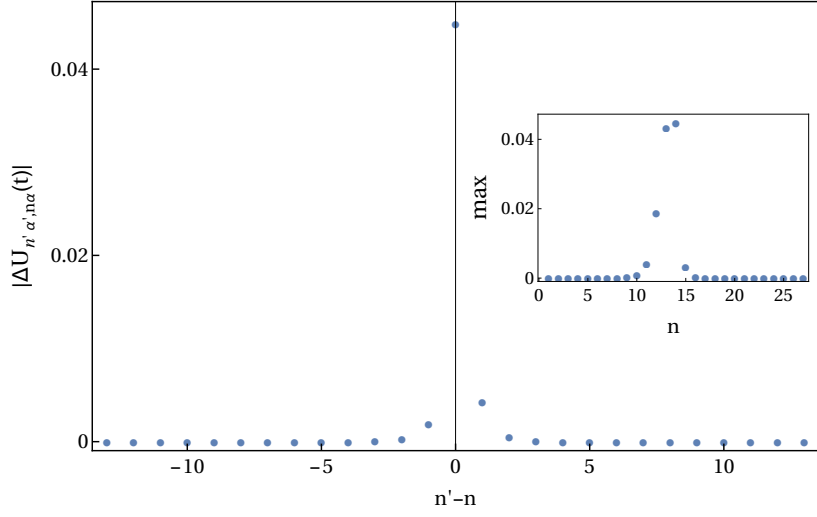


FIG. 7: Numerical check that localized disorder does not spread under the loop decomposition. We consider the model described in the main text with system size $L = 27$, parameters $h_1 = 0.9, h_2 = 1.62, T_{\text{drive}} = 2\pi, t = T_{\text{drive}}/2 + 0.01, h_d = 0.2$, and the defect site $n_0 = 13$. We fix $\alpha = \alpha' = A$, but similar results were obtained for other values. In the main plot, we set $n = 14$. The inset plots the quantity (C6), which is maximal at $n = 14$.

Appendix D: Reflection amplitude starts at linear order

Consider the scattering problem as defined in Sec. IV, with a disordered region of size N connected to clean leads, at some arbitrary Δt . In this section, we use the notation

$$U_0 = U_{\text{clean}}(T_{\text{drive}}/2), \quad (\text{D1a})$$

$$\tilde{U} = U(T_{\text{drive}}/2), \quad (\text{D1b})$$

$$U = U(T_{\text{drive}}/2 + \Delta t), \quad (\text{D1c})$$

and we also write

$$\tilde{U} = U_0 + \tilde{V}, \quad (\text{D2a})$$

$$U = U_0 + \tilde{V} + V, \quad (\text{D2b})$$

where the disorder terms V and \tilde{V} are exponentially localized to the sample region (the sites $1, \dots, N$).

Our task is to show the following: If the scattering problem for \tilde{U} has zero reflection, then the scattering problem for U has reflection that generically starts at linear order in V . This suffices because V generically starts at linear order in Δt [see Eq. (2.22)].

We now proceed using the general scattering framework developed in Ref. [46] for discrete-time problems. Consider an eigenstate $|\Psi\rangle$ of U_0 with some definite momentum (either right-moving or left-moving) and eigenvalue $e^{-i\omega}$. The corresponding scattering “in” states for \tilde{U} and U satisfy the appropriate Lippmann-Schwinger equation:

$$|\tilde{\Psi}_{\text{in}}\rangle = |\Psi\rangle + G_0 \tilde{V} |\tilde{\Psi}_{\text{in}}\rangle, \quad (\text{D3a})$$

$$|\Psi_{\text{in}}\rangle = |\Psi\rangle + G_0 (\tilde{V} + V) |\Psi_{\text{in}}\rangle, \quad (\text{D3b})$$

where $G_0 = (e^{-i(\omega+i0^+)} - U_0)^{-1}$ is the free Green’s function [46]. Indeed, Eqs. (D3a) and (D3b) follow from Eq. (S.3) from the Supplemental Material of Ref. [46] and the relation $|\Psi_{\text{in}}\rangle = \Omega_+ |\Psi\rangle$ (see also their footnote 53).

A similar equation relating the two scattering states is then readily obtained:

$$|\Psi_{\text{in}}\rangle = |\tilde{\Psi}_{\text{in}}\rangle + \tilde{G} V |\Psi_{\text{in}}\rangle, \quad (\text{D4})$$

where $\tilde{G} = (e^{-i(\omega+i0^+)} - \tilde{U})^{-1}$ is the Green’s function of \tilde{U} . Expanding in V , we get

$$|\Psi_{\text{in}}\rangle = |\tilde{\Psi}_{\text{in}}\rangle + \tilde{G} V |\tilde{\Psi}_{\text{in}}\rangle + O(V^2). \quad (\text{D5})$$

By assumption, $|\tilde{\Psi}\rangle$ has zero reflection, i.e., its wavefunction agrees with that of $|\Psi\rangle$ for $n \rightarrow -\infty$ (assuming for definiteness that $|\Psi\rangle$ is right-moving). The term linear in V generically has nonvanishing amplitude for $n \rightarrow -\infty$, thus yielding the reflection amplitude $(r_{1\dots N})$ starting at linear order in V .

-
- [1] B. Huckestein, Scaling theory of the integer quantum Hall effect, *Reviews of Modern Physics* **67**, 357 (1995).
- [2] B. I. Halperin, Quantized Hall conductance, current-carrying edge states, and the existence of extended states in a two-dimensional disordered potential, *Physical Review B* **25**, 2185 (1982).
- [3] M. Ippoliti and R. N. Bhatt, Dimensional Crossover of the Integer Quantum Hall Plateau Transition and Disordered Topological Pumping, *Physical Review Letters* **124**, 086602 (2020).
- [4] A. Kitaev, Periodic table for topological insulators and superconductors, *AIP Conference Proceedings* **1134**, 22 (2009).
- [5] V. Kagalovsky and D. Nemirovsky, Universal Critical Exponent in Class D Superconductors, *Physical Review Letters* **101**, 127001 (2008).
- [6] F. Evers and A. D. Mirlin, Anderson transitions, *Reviews of Modern Physics* **80**, 1355 (2008).
- [7] J. Song and E. Prodan, AIII and BDI topological systems at strong disorder, *Physical Review B* **89**, 224203 (2014).
- [8] J. Song, C. Fine, and E. Prodan, Effect of strong disorder on three-dimensional chiral topological insulators: Phase diagrams, maps of the bulk invariant, and existence of topological extended bulk states, *Physical Review B* **90**, 184201 (2014).
- [9] I. Mondragon-Shem, T. L. Hughes, J. Song, and E. Prodan, Topological Criticality in the Chiral-Symmetric AIII Class at Strong Disorder, *Physical Review Letters* **113**, 046802 (2014).
- [10] Z. Xiao, K. Kawabata, X. Luo, T. Ohtsuki, and R. Shindou, Anisotropic Topological Anderson Transitions in Chiral Symmetry Classes, *Physical Review Letters* **131**, 056301 (2023).
- [11] A. Altland, D. Bagrets, and A. Kamenev, Topology versus Anderson localization: Nonperturbative solutions in one dimension, *Physical Review B* **91**, 085429 (2015).
- [12] T. Morimoto, A. Furusaki, and C. Mudry, Anderson localization and the topology of classifying spaces, *Physical Review B* **91**, 235111 (2015).
- [13] P. Titum, N. H. Lindner, M. C. Rechtsman, and G. Refael, Disorder-Induced Floquet Topological Insulators, *Physical Review Letters* **114**, 056801 (2015).
- [14] S. Roy and G. J. Sreejith, Disordered Chern insulator with a two-step Floquet drive, *Physical Review B* **94**, 214203 (2016).
- [15] P. Titum, N. H. Lindner, and G. Refael, Disorder-induced transitions in resonantly driven Floquet topological insulators, *Physical Review B* **96**, 054207 (2017).
- [16] H. Obuse and N. Kawakami, Topological phases and delocalization of quantum walks in random environments, *Physical Review B* **84**, 195139 (2011).
- [17] T. Kitagawa, Topological phenomena in quantum walks: Elementary introduction to the physics of topological phases, *Quantum Information Processing* **11**, 1107 (2012).
- [18] T. Rakovszky and J. K. Asboth, Localization, delocalization, and topological phase transitions in the one-dimensional split-step quantum walk, *Physical Review A* **92**, 052311 (2015).
- [19] I. Vakulchyk, M. V. Fistul, P. Qin, and S. Flach, Anderson localization in generalized discrete-time quantum walks, *Physical Review B* **96**, 144204 (2017).
- [20] S. Derevyanko, Anderson localization of a one-dimensional quantum walker, *Scientific Reports* **8**, 1795 (2018).
- [21] T. Kitagawa, M. S. Rudner, E. Berg, and E. Demler, Exploring topological phases with quantum walks, *Physical Review A* **82**, 033429 (2010).
- [22] O. Shtanko and R. Movassagh, Stability of Periodically Driven Topological Phases against Disorder, *Physical Review Letters* **121**, 126803 (2018).
- [23] M. M. Wauters, A. Russomanno, R. Citro, G. E. Santoro, and L. Privitera, Localization, Topology, and Quantized Transport in Disordered Floquet Systems, *Physical Review Letters* **123**, 266601 (2019).
- [24] Y. Gannot, Effects of Disorder on a 1-D Floquet Symmetry Protected Topological Phase, [arXiv:1512.04190](https://arxiv.org/abs/1512.04190).
- [25] Here and throughout, our Hamiltonians and unitary time evolutions refer to single-particle matrices, not to the corresponding multiparticle operators that act on Fock space. Thus, \mathcal{C} is unitary rather than antiunitary [48].
- [26] F. Harper, R. Roy, M. S. Rudner, and S. Sondhi, Topology and Broken Symmetry in Floquet Systems, *Annual Review of Condensed Matter Physics* **11**, 345 (2020).
- [27] R. Roy and F. Harper, Periodic table for Floquet topological insulators, *Physical Review B* **96**, 155118 (2017).
- [28] X. Liu, F. Harper, and R. Roy, Chiral flow in one-dimensional Floquet topological insulators, *Physical Review B* **98**, 165116 (2018).
- [29] In particular, $L_{loc}(t)$ is the localization length for the time-periodic Floquet states of the operator $U_{loop}(t)$ considered as if t were the full period.
- [30] A. Brown, *Geometric Current Response in Chern Systems and Topological Delocalization in Floquet Class AIII Systems*, Ph.D. thesis, UCLA (2019).
- [31] P. S. Sathe, *Aspects of Localization in Topological Insulators*, Ph.D. thesis, UCLA (2023).
- [32] G. M. Graf and C. Tauber, Bulk-Edge Correspondence for Two-Dimensional Floquet Topological Insulators, *Annales Henri Poincaré* **19**, 709 (2018).
- [33] A. Kitaev, Anyons in an exactly solved model and beyond, *Annals of Physics* **321**, 2 (2006).
- [34] D. Gross, V. Nesme, H. Vogts, and R. F. Werner, Index Theory of One Dimensional Quantum Walks and Cellular Automata, *Communications in Mathematical Physics* **310**, 419 (2012).
- [35] D. Ranard, M. Walter, and F. Witteveen, A Converse to Lieb-Robinson Bounds in One Dimension Using Index

- Theory, *Annales Henri Poincaré* **23**, 3905 (2022).
- [36] P. Sathe, A. B. Culver, R. Pandey, and R. Roy, (unpublished).
- [37] T. Liu, X. Xia, S. Longhi, and L. Sanchez-Palencia, Anomalous mobility edges in one-dimensional quasiperiodic models, *SciPost Physics* **12**, 027 (2022).
- [38] R. Schrader, H. Schulz-Baldes, and A. Sedrakyán, Perturbative Test of Single Parameter Scaling for 1D Random Media, *Annales Henri Poincaré* **5**, 1159 (2004).
- [39] W. P. Su, J. R. Schrieffer, and A. J. Heeger, Solitons in Polyacetylene, *Physical Review Letters* **42**, 1698 (1979).
- [40] M. S. Rudner, N. H. Lindner, E. Berg, and M. Levin, Anomalous Edge States and the Bulk-Edge Correspondence for Periodically Driven Two-Dimensional Systems, *Physical Review X* **3**, 031005 (2013).
- [41] R. Resta, Quantum-Mechanical Position Operator in Extended Systems, *Physical Review Letters* **80**, 1800 (1998).
- [42] A. B. Culver, P. Sathe, and R. Roy, Scattering expansion for localization in one dimension, *Physical Review B* **109**, L060201 (2024).
- [43] A. B. Culver, P. Sathe, and R. Roy, Scattering expansion for localization in one dimension: From disordered wires to quantum walks, *Physical Review B* **109**, 064201 (2024).
- [44] This formula is based on assumptions that can be expected to hold for “generic” disorder distributions and model parameters. The $O(|r_j|^3)$ can in fact be replaced by $O(|r_j|^4)$ (i.e., the third-order terms vanish), as discussed in Refs. [42] and [43]; however, only the second-order terms are important for our present goal of showing $\nu = 2$.
- [45] P. W. Anderson, D. J. Thouless, E. Abrahams, and D. S. Fisher, New method for a scaling theory of localization, *Physical Review B* **22**, 3519 (1980).
- [46] A. Bisio, N. Mosco, and P. Perinotti, Scattering and Perturbation Theory for Discrete-Time Dynamics, *Physical Review Letters* **126**, 250503 (2021).
- [47] I. C. Fulga, B. van Heck, J. M. Edge, and A. R. Akhmerov, Statistical topological insulators, *Physical Review B* **89**, 155424 (2014).
- [48] C.-K. Chiu, J. C. Y. Teo, A. P. Schnyder, and S. Ryu, Classification of topological quantum matter with symmetries, *Reviews of Modern Physics* **88**, 035005 (2016).